

Combined Experimental and Computational Study on Ruthenium(II)-Catalyzed Reactions of Diynes with Aldehydes and *N,N*-Dimethylformamide

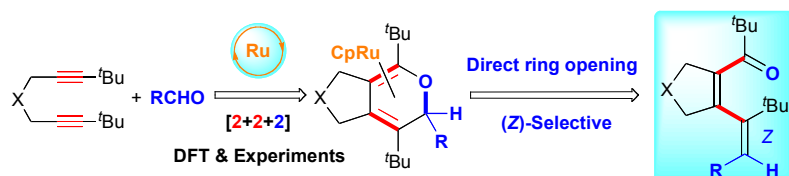
Yoshihiko Yamamoto,* Yuta Okude, Shota Mori, and Masatoshi Shibuya

Department of Basic Medicinal Sciences, Graduate School of Pharmaceutical Sciences,

Nagoya University, Chikusa, Nagoya 464-8601, Japan

*yamamoto-yoshi@ps.nagoya-u.ac.jp

In memory of Prof. Takao Ikariya.



Abstract: Cycloaddition reactions of 1,6-diynes bearing methyl terminal groups with

p-anisaldehyde were conducted using a cationic ruthenium catalyst with a η^5 -pentamethylcyclopentadienyl ligand in THF at room temperature to afford dienyl ketones *via* ring opening of the initially formed fused pyrans. (*Z*)-Stereoisomers of dienyl ketones were selectively obtained using the ruthenium catalyst, whereas previously reported rhodium catalysts produced (*E*)-isomers. These (*E*)- and (*Z*)-selectivities are kinetically controlled as the control experiments showed that the *E/Z*-isomerization of (*E*)-dienylketone occurs at 70 °C for 10 h to afford an *E/Z* ratio of almost 1:1. The origin of this characteristic stereoselectivity for the ruthenium catalyst was attributed to the direct ring opening of the CpRu^+ -coordinated pyran complex intermediates on the basis of theoretical calculations [PCM (THF) M06L/SDD-6-31++G(d,p)//B3LYP/LanL2DZ-6-31G(d)] and control experiments. The (*Z*)-selectivity increased when the bulkiness of the diyne terminal substituents increased. Notably, the reaction of 1,6-diyne bearing *tert*-butyl terminal groups with various α,β -unsaturated aldehydes exclusively afforded (*Z*)-dienyl ketones even at 70 °C when a cationic ruthenium complex with a smaller η^5 -cyclopentadienyl (Cp) ligand was used as the catalyst. The same Cp complex was found to be also efficient for the

hydrocarbamoylative cyclization of sterically demanding 1,6-diynes bearing tertiary or quaternary carbon tethers with *N,N*-dimethylformamide.

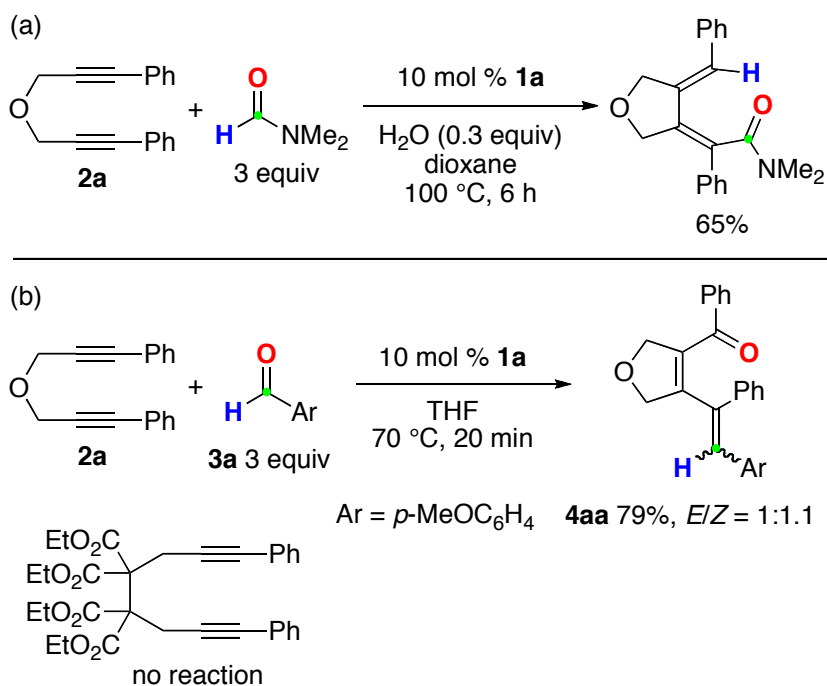
Introduction

The transition-metal-catalyzed [2 + 2 + 2] cycloaddition of alkynes has been known as a powerful tool for single-step assembly of highly substituted benzenes.¹ Similarly, the [2 + 2 + 2] cocycloadditions of alkynes with nitriles or isocyanates produce valuable nitrogen heterocycles such as pyridines and pyridones.² In contrast, relevant cycloadditions of alkynes with carbonyl compounds have been significantly less developed owing to the weak coordination ability of carbonyl groups compared to that of soft nitrogen compounds such as nitriles or isocyanates. For example, Tsuda, Saegusa, and coworkers pioneered nickel-catalyzed cycloadditions of α,ω -diynes with aldehydes, leading to fused pyrans and their ring-opened derivatives.^{3a} Later, Tekevac and Louie expanded the scope of this reaction in terms of the carbonyl partner to ketones using an *N*-heterocyclic carbene ligand.^{3b} Although several stoichiometric reactions using cobalt and zirconium complexes were also reported,⁴ catalytic protocols

have long been limited to nickel catalysts. Recently, the Shibata and Tanaka laboratories have independently developed rhodium-catalyzed methods.^{5,6} In particular, Tanaka and coworkers expanded the scope of carbonyl compounds: in addition to simple aldehydes and ketones, the authors successfully employed dicarbonyl compounds and acylphosphonates as the cycloaddition partners.^{5b} Our group reported ruthenium-catalyzed cycloadditions of 1,6-diyne with electron-deficient ketones.⁷ In this previous study, however, only tricarbonyl compounds functioned as the carbonyl components in the presence of a neutral ruthenium catalyst, Cp*RuCl(cod) (Cp* = η^5 -C₅Me₅, cod = 1,5-cyclooctadiene).

We recently discovered that hydrocarbamoylative cyclization of 1,6-diyne bearing phenyl terminal groups with *N,N*-dimethylformamide (DMF) proceeds in the presence of a cationic ruthenium catalyst, [Cp*Ru(MeCN)₃]⁺PF₆⁻ (**1a**) (Scheme 1a).⁸ This reaction mode is different from those of previous [2 + 2 + 2] cycloaddition reactions of diynes with aldehydes and ketones because the formyl C–H bond is cleaved. To extend this work further, we screened formyl compounds such as formate esters and aldehydes, and found that reaction of diyne **2a** with *p*-anisaldehyde (**3a**) produces **4aa** as a result of

normal [2 + 2 + 2] cycloaddition/electrocyclic ring opening (Scheme 1b). Although the yield was good (79%), the stereochemistry of the resultant 1,2-diarylalkene moiety was not controlled ($E/Z = 1:1.1$). This lack of stereoselectivity is in striking contrast to those typically reported for rhodium-catalyzed cycloadditions of similar diynes, bearing alkyl terminal groups, with aldehydes.⁵ Therefore, we reasoned that the stereoselectivity might depend on the substrate structure and/or reaction conditions. Herein, we report the results of our combined experimental and computational study on the ruthenium-catalyzed reaction of diynes, equipped with alkyl terminal groups, with aldehydes, in which stereoselectivity differed markedly from that observed in previously reported rhodium-catalyzed reactions. In addition, hydrocarbamoylative cyclization of previously challenging 1,6-diyne substrates was revisited using a different catalyst.



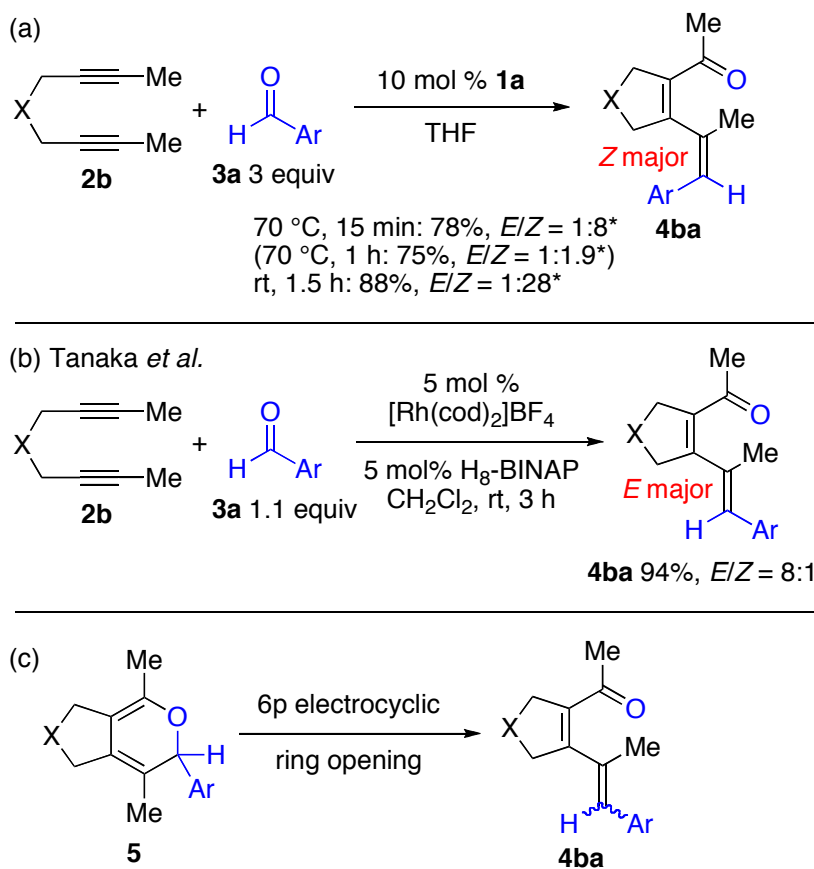
Scheme 1. Ruthenium-catalyzed reactions of diyne **2a** with (a) DMF and (b) aldehyde

(**2a**).

Results and Discussion

Initial experimental results and a proposed mechanism for the reaction of 1,6-diynes with aldehydes. As mentioned above, the reaction of **2a** with **3a** afforded dienyl ketone **4aa** in a good yield but without stereoselectivity. In addition, the reaction was found to be limited to 1,6-diynes as the 1,7-diyne with phenyl terminal groups and two malonate moieties in the tether was completely unreactive (Scheme 1b). Thus, we turned our attention to 1,6-diynes with alkyl terminal groups as substrates. At the outset,

the reaction of malonate-derived diyne **2b**, bearing methyl terminal groups, with **3a** was performed and the stereoselectivity of the obtained product **4ba** was compared with that reported previously (Scheme 2). Tanaka and coworkers reported that the reaction of **2b** with **3a** proceeded at room temperature in the presence of 5 mol % [Rh(cod)₂]BF₄ and H₈-BINAP ligand to afford (*E*)-**4ba** as the major stereoisomer in an excellent yield (Scheme 2b).^{5b} In contrast, when the same reaction was conducted using 10 mol % **1a** as the catalyst in THF at 70 °C for 15 min, **4ba** was produced in 78% yield with the opposite stereoselectivity (*E/Z* = 1:8) (Scheme 2a). Furthermore, an improved yield (88%) and stereoselectivity (*E/Z* = 1:28) were observed, when the same reaction was performed at room temperature, albeit for a longer time of 1.5 h. Thus, these results suggest that the stereoselectivity in the formation of the ring-opened product depends on both substrate structure (Schemes 1b vs. 2a) and reaction conditions (Schemes 2a vs. 2b).



Scheme 2. (a) Ruthenium- and (b) rhodium-catalyzed reactions of diyne **2b** with aldehyde **3a**, and (c) 6π electrocyclic ring opening of the initially formed bicyclic pyran **5**. X = C(CO₂Me)₂, Ar = *p*-MeOC₆H₄. **E/Z* ratio for crude products.

As previously reported,^{4,5,7} it is believed that the initial product of the [2 + 2 + 2] cycloaddition of diyne **2b** with aldehyde **3a** is bicyclic pyran **5**, which undergoes thermal electrocyclic ring opening to produce dienyl ketone **4ba** (Scheme 2c). According to this mechanism, the stereoselectivity in the formation of **4ba** is

determined during the pyran ring-opening step: the stereochemistry of **4ba** can be controlled by the kinetic preference for one of the two rotatory directions of the aryl group (torquoselectivity)⁹ and/or the thermodynamic stability of (*E*)- and (*Z*)-**4ba**. Thus, density functional theory (DFT) calculations were performed at the PCM (THF) M06L/SDD-6-31++G(d,p)//B3LYP/LanL2DZ-6-31G(d) level of theory to inspect the electrocyclic ring opening of a model pyran (Figure 1). For computational efficiency, tetrahydrofuran-fused pyran **A** was selected as the model compound. The starting pyran **A** can adopt two conformations: the phenyl substituent can occupy an equatorial position (*eq*-**A**) or axial position (*ax*-**A**). The former is slightly (0.7 kcal/mol) less stable than the latter owing to the steric repulsion between methyl and phenyl substituents. The transition states (TSs) for the outward and inward rotations were located higher in energy by 11.8 and 13.5 kcal/mol, respectively, than *ax*-**A**. In contrast, the dienyl ketone (*Z*)-**B** was estimated to be 2.2 kcal/mol more stable than (*E*)-**B**. Accordingly, the outward-rotation product (*E*)-**B** is kinetically favored with the estimated *E/Z* ratio of 18:1. On the other hand, the inward-rotation product (*Z*)-**B** is thermodynamically favored and the calculated equilibrium *E/Z* ratio is 1:42. Calculations for the ring

opening of the real compound **5** also afforded a similar energy profile as shown in

Figure 1.

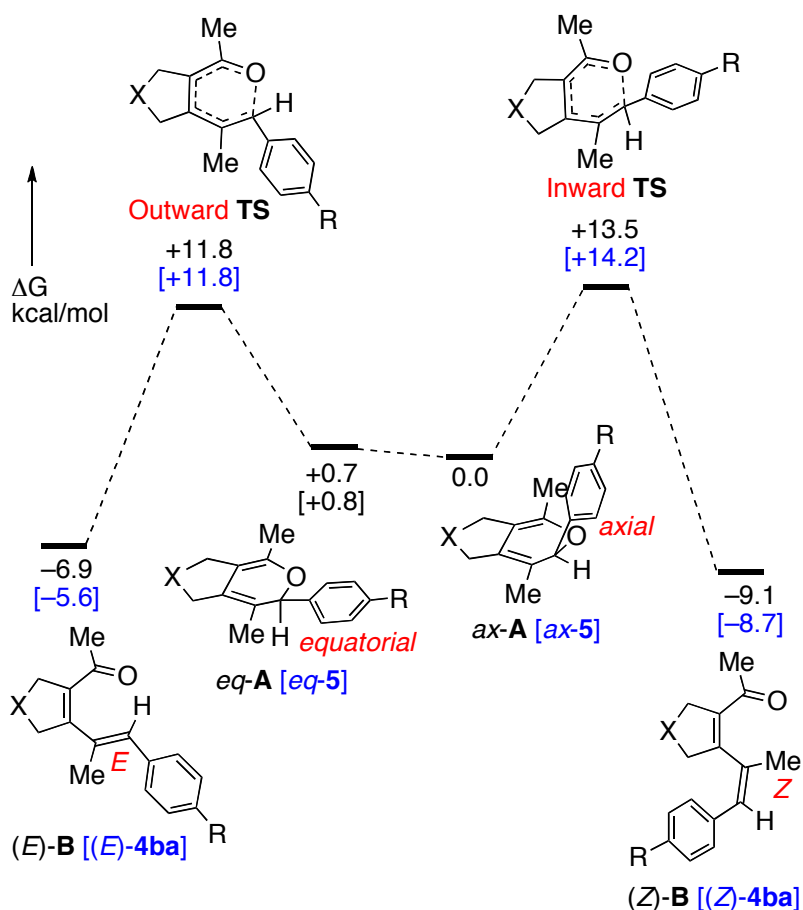


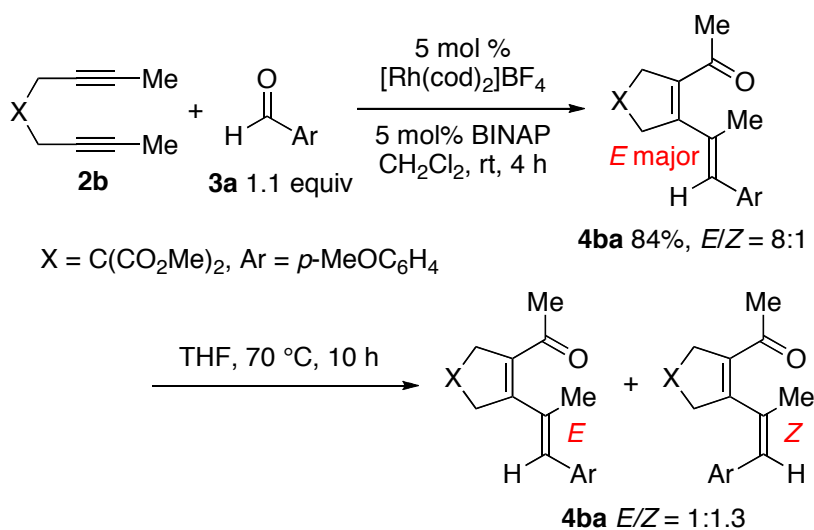
Figure 1. Calculated energy surface for the electrocyclic ring opening of a model pyran

A and malonate derivative **5** ($X = C(\text{CO}_2\text{Me})_2$, $R = \text{OMe}$) with relative Gibbs free

energies in THF at 298 K, 1 atm [PCM (THF) M06L/SDD-

6-31++G(d,p)//B3LYP/LanL2DZ-6-31G(d)].

Taking into consideration the above computational data, the results shown in Scheme 2 can be interpreted as follows: the rhodium-catalyzed reaction proceeds at room temperature to generate the kinetically more favored (*E*)-**4ba** as the major stereoisomer, while the ruthenium-catalyzed reaction affords the thermodynamically more favored (*Z*)-**4ba** as the major stereoisomer. However, the *E/Z* ratio (1:28 at rt) for the ruthenium catalyzed reaction is much higher than that expected according to the above calculations. The *E/Z* ratio was lower (1:8) at 70 °C and further lowered after a longer reaction time for 1 h (Scheme 2a, shown in parentheses). These facts show that the initially formed product (*Z*)-**4ba** is gradually converted into (*E*)-**4ba** at 70 °C. To check thermal *E/Z* isomerization, **4ba**, which was obtained by the rhodium/BINAP-catalyzed reaction with an *E/Z* ratio of 8:1,^{5a} was heated in THF at 70 °C for 10 h (Scheme 3). As a result, the *E/Z* ratio of the recovered **4ba** decreased to 1:1.3. Therefore, the formation of **4ba** from pyran **5** is reversible and the equilibrium *E/Z* ratio is 1:1.3 at 70 °C.



Scheme 3. Synthesis of (*E*)-**4b** and its thermal isomerization to (*Z*)-**4b**.

Computational study on the ruthenium-catalyzed [2 + 2 + 2] cycloaddition of a model diyne with benzaldehyde. It has been suggested that ruthenium-catalyzed [2 + 2 + 2] alkyne cyclotrimerization and the relevant cocycloadditions involving other unsaturated molecules proceed via the oxidative coupling of alkynes with $[\text{Cp}'\text{RuCl}]$ fragments and subsequent [2 + 2] cycloaddition of the resultant ruthenacyclopentatrienes with the third reaction component.¹⁰ In order to gain insights into the (*Z*)-selectivity observed in the ruthenium catalysis, the reaction of model ruthenium diyne complex **C** ligated by benzaldehyde was analyzed by DFT calculations (Figure 2 and Figure S1 in Supporting Information). The initial oxidative cyclocoupling

of the diyne ligand with the CpRu⁺ fragment proceeded with an activation energy of +12.7 kcal/mol, generating ruthenacyclopentadiene **D**. Ruthenacycle **D** underwent facile isomerization to ruthenacyclopentatrienes *exo*-**E** via **TS_{DE}** with a small activation energy of +6.9 kcal/mol. Due to its delocalized structure, *exo*-**E** is 13 kcal/mol more stable than **D**.

There are two major stereochemical courses available for the subsequent [2 + 2] cycloaddition. The first is an *endo* mode, where the aldehyde phenyl substituent is oriented towards the ruthenacycle moiety, and the other is the *exo* mode with the opposite phenyl orientation. The activation energy was found to be 1.9 kcal/mol lower for the *endo* transition state (*endo*-**TS_{EF}**) than for *exo*-**TS_{EF}**. The formation of ruthenatricycle intermediates with long Ru-C α distances (2.248 and 2.319 Å, respectively) was more endergonic for *exo*-**F** than for *endo*-**F**. Therefore, the initial [2 + 2] cycloaddition step is more feasible for the *endo* mode than for the *exo* mode. Notably, *exo/endo*-**F** have distorted three-legged piano-stool geometry with the C α' -O* distances of ca. 3.12 Å and therefore, subsequent C α' -O* bond-forming reductive elimination readily occurred to produce η^4 -pyran complexes *exo/endo*-**G**. The

activation energy was found to be 1.7 kcal/mol lower for *endo*-**TS_{FG}** than for *exo*-**TS_{FG}**.

The formations of *endo/exo*-**G** were largely exergonic owing to the stability of η^4 -diene complexes. More importantly, the DFT calculations showed that both pyran complexes can evolve into ring-opened products (*E*)/(*Z*)-**H** with smaller activation energies than those associated with the ring opening of the corresponding free pyran **A** (Figure 1).

Notably, upon coordination, the C*-O* bonds were elongated by 0.066 Å for *endo*-**G/ax-A** and 0.068 Å for *exo*-**G/eq-A**, thereby facilitating the ring opening step.

Therefore, it can be qualitatively assumed that the kinetically more favored *endo* pathway directly delivered the (*Z*)-dienyl ketone as the kinetic product under the ruthenium-catalyzed conditions. The most highest energy barrier estimated for the initial oxidative cyclocoupling process from **C** is lower than 20 kcal/mol and the production of the final dienyl ketone complexes **H** from **C** is ca. 50 kcal/mol exergonic.

Thus, the overall catalytic process should be feasible at room temperature.

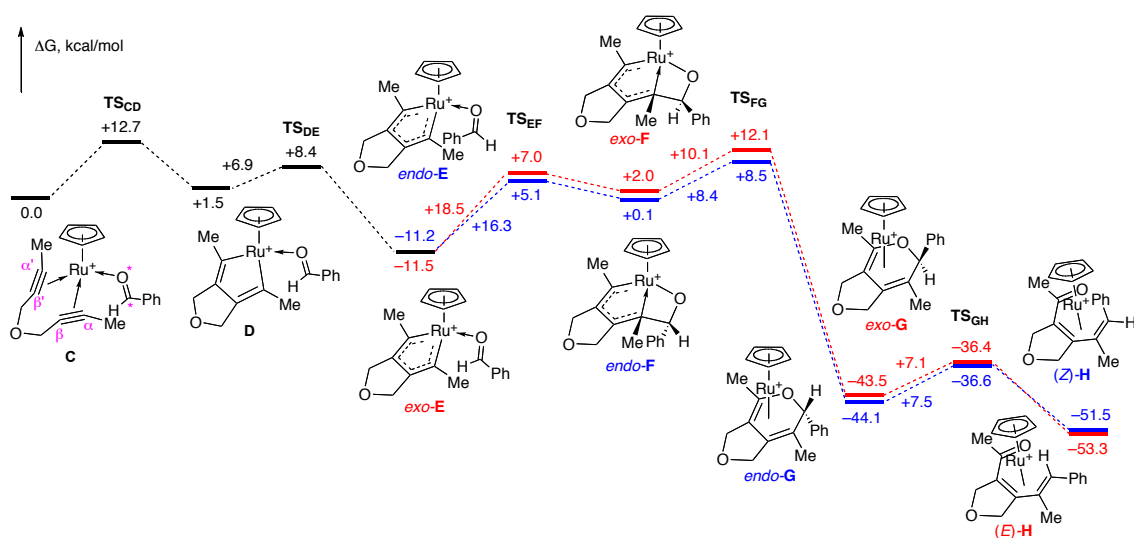
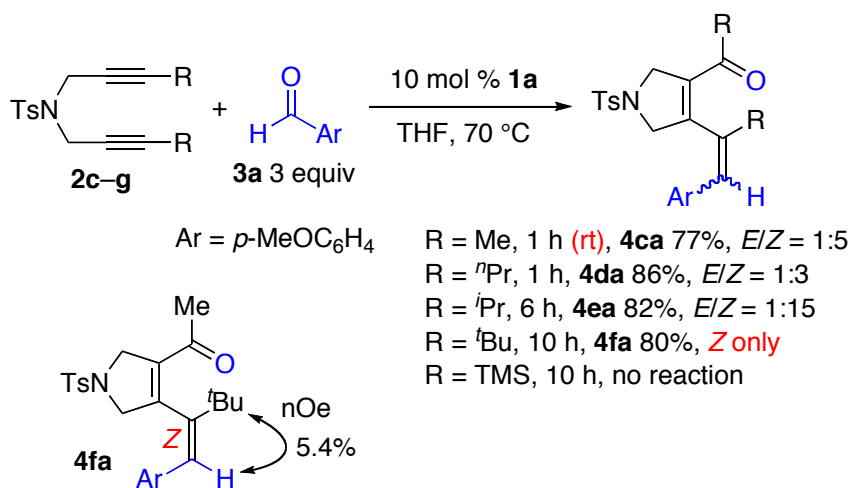


Figure 2. Calculated energy surface for the reaction of model complex **C** leading to (*E*)- and (*Z*)-dienyl ketone complexes **H** with relative Gibbs free energies in THF at 298 K, 1 atm [PCM (THF) M06L/SDD-6-31++G(d,p)//B3LYP/LanL2DZ-6-31G(d), *endo*-mode, blue; *exo*-mode, red].

Scope and limitations of the ruthenium-catalyzed reaction of 1,6-diyne with aldehydes. In the next step, we investigated the influence of the diyne terminal alkyl groups. For ease of separation, tosylamide-derived diynes bearing methyl, *n*-propyl, isopropyl, and *tert*-butyl terminal groups were selected as substrates (Scheme 4). The reaction of diyne **2c** bearing methyl substituents with aldehyde **3a** was completed within 1 h using 10 mol % **1a** in THF at room temperature, affording **4ca** in 77% yield. The ^1H

NMR analysis of crude **4ca** revealed that the *E/Z* ratio (1:5) was lower than that for **4ba** (1:28). Therefore, the stereoselectivity depends on the tether groups. The reactions of other diyne substrates bearing bulkier terminal substituents required elevated reaction temperatures, due to sluggish reactions. When the reaction of diyne **2d** bearing *n*-propyl substituents with aldehyde **3a** was conducted at 70 °C for 1 h, **4da** was obtained in 86% yield with an *E/Z* ratio of 1:3. Further increase in the bulkiness of the diyne terminal substituents provided a positive effect on the stereoselectivity. Namely the use of diyne **2e** bearing isopropyl substituents led to the formation of **4ea** in 82% yield with a significantly improved *E/Z* ratio of 1:15, even though a longer reaction time of 6 h was required for the reaction to reach completion. Furthermore, only the (*Z*)-isomer was produced when diyne **2f** bearing *tert*-butyl substituents was examined. However, in this case, the reaction was not complete even after 10 h and 16% of **2f** remained unreacted. In striking contrast, no reaction occurred when diyne **2g** bearing trimethylsilyl (TMS) terminal groups was used as the substrate. The stereochemistry of **4fa** was confirmed by nuclear Overhauser effect (nOe) observed between the *tert*-butyl group and vinylic proton on the alkene moiety.



Scheme 4. Reactions of diynes **2c–g** with aldehyde **3a**.

The above results imply that dienyl ketone (*Z*)-**4fa**, bearing *tert*-butyl substituents, was irreversibly produced and the isomerization to give the (*E*)-isomer was completely suppressed. To examine this behavior further, DFT calculations were repeated for the ring opening reaction of model pyran **I** (Figure 3). Among the two possible conformers, *eq*-**I** was found to be 7.8 kcal/mol less favored than *ax*-**I** owing to the severe steric repulsion between the *tert*-butyl and phenyl groups. The transition state for the outward rotation and the product (*E*)-**J** were located 1.3 and 4.4 kcal/mol higher than the transition state for the inward rotation and (*Z*)-**J**, respectively. Therefore, the formation

of the (*Z*)-isomer is both kinetically and thermodynamically favored. Moreover, the activation energy of the ring closing of (*Z*)-**J** was estimated to be 26.3 kcal/mol. This value is higher than that calculated for the ring closing of (*Z*)-**B** (22.6 kcal/mol). Accordingly, the *E/Z* isomerization is effectively suppressed.

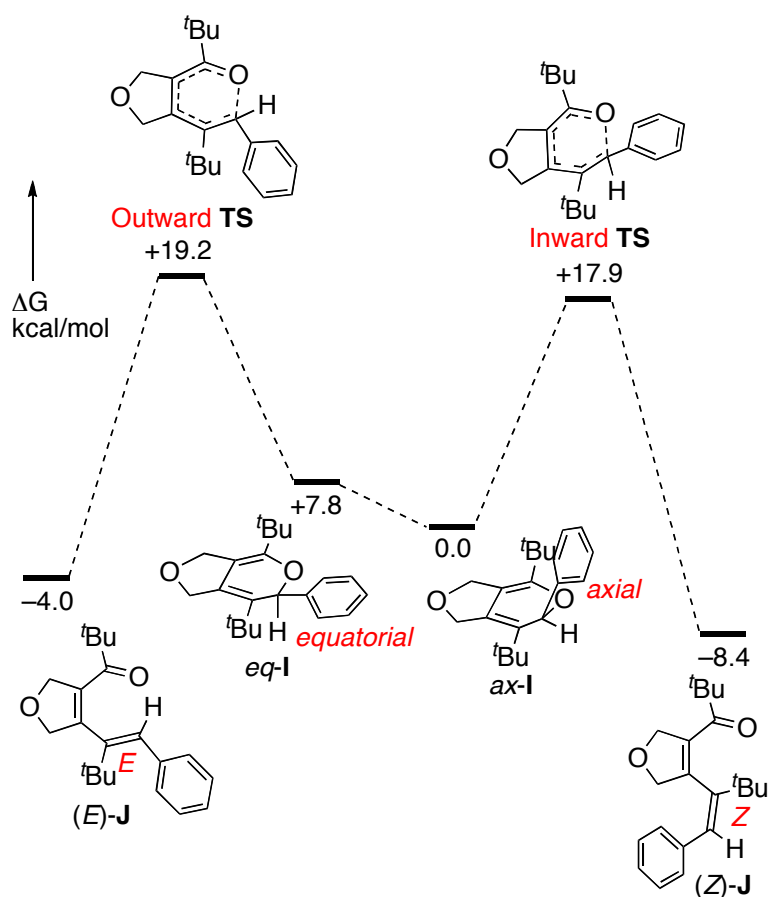
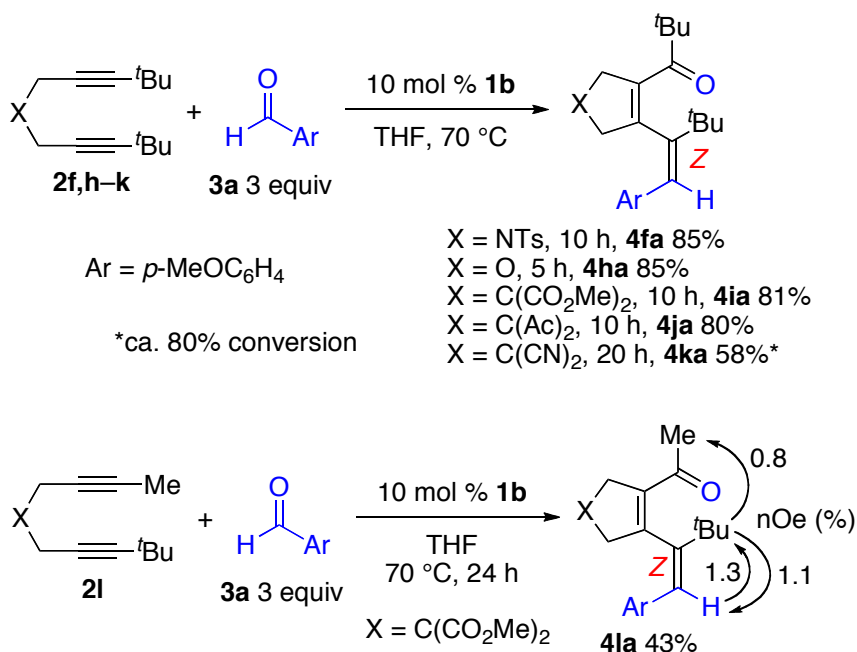


Figure 3. Calculated energy surface for the electrocyclic ring opening of a model pyran **I** with relative Gibbs free energies in THF at 298 K, 1 atm [PCM (THF) M06L/SDD-6-31++G(d,p)//B3LYP/LanL2DZ-6-31G(d)].

Next, the influence of the tether moiety was investigated using diynes bearing *tert*-butyl terminal groups (Scheme 5). Previous experiments showed that the reaction of bulky diyne **2f** was not complete even within 10 h and therefore, we employed a cationic ruthenium complex bearing a smaller Cp ligand, [CpRu(MeCN)₃]PF₆ (**1b**, Cp = η⁵-C₅H₅), as the catalyst. Thus, in the presence of 10 mol % **1b**, the reaction of **2f** with **3a** in THF at 70 °C was complete within 10 h, affording **4fa** in 85% yield. Similarly, ether-tethered diyne **2h** underwent cycloaddition with **3a** in a shorter reaction time of 5 h, affording **4ha** in 85% yield. These new conditions were found to be effective also for diynes bearing a quaternary carbon center: **4ia** and **4ja** were obtained in 81% and 80% yields, respectively, from the reactions of malonate- or acetylacetonone-derived diynes **2i** and **2j** within 10 h. Moreover, the reaction of malononitrile-derived diyne **2k** afforded **4ka** in 58% yield, although the reaction did not reach completion even after 20 h. Accordingly, the formyl group of **3a** exclusively reacted in the presence of esters, ketones, and nitriles under the reaction conditions employing the cationic ruthenium catalyst (see below). The known unsymmetrical diyne **2l** bearing methyl and *tert*-butyl

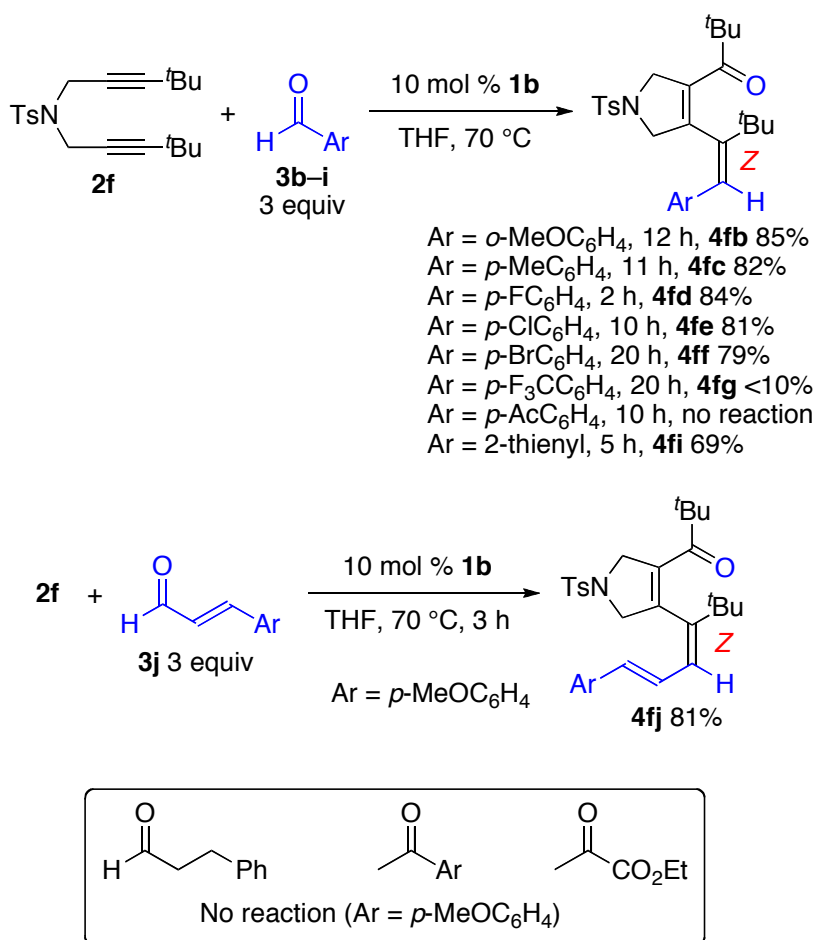
terminal groups was also used as a substrate to investigate regioselectivity.¹¹ The reaction of **2l** with **3a** was sluggish with only 83% conversion of **2l** even after heating for 24 h and a modest yield of **4la** (43%). Nevertheless, **4la** was obtained as an exclusive regio- and stereoisomer as confirmed by nOe measurements.



Scheme 5. Reactions of diynes **2f,h-l** with aldehyde **3a**.

Finally, the scope of the carbonyl components was investigated for the reaction with diyne **2f** (Scheme 6). The reaction with *o*-anisaldehyde (**3b**) was slower than that with *p*-anisaldehyde (**3a**), most likely as a result of the steric effect. When

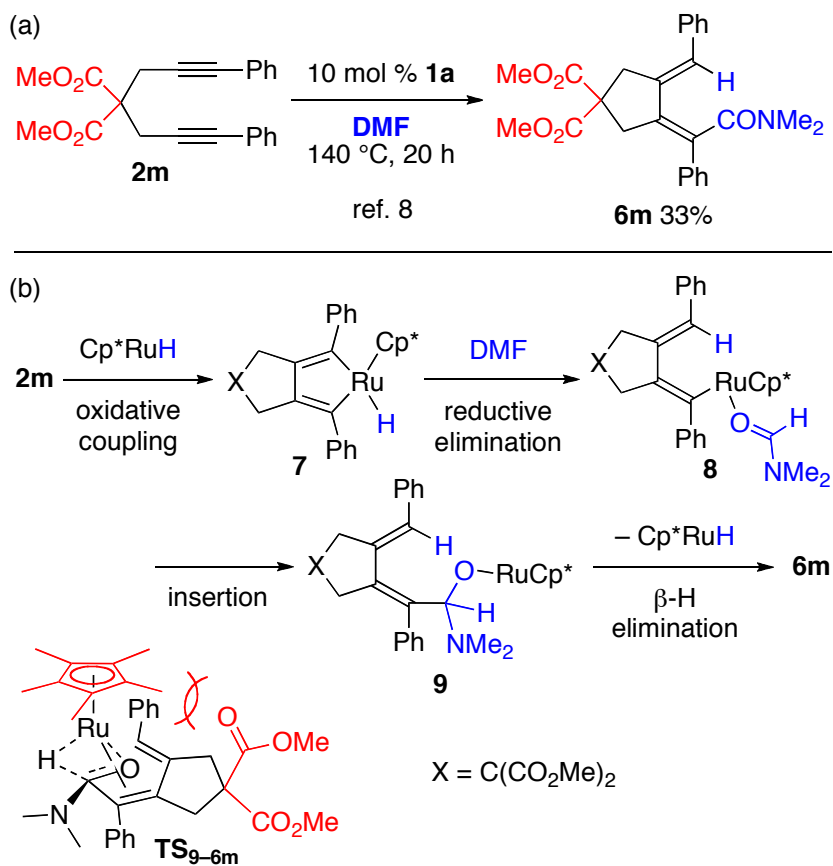
p-tolualdehyde (**3c**) was used, the corresponding adduct **4fc** was obtained in 82% yield. Benzaldehydes **3d–f**, bearing F, Cl, and Br substituents at the *para*-position, were also used to obtain the corresponding products in good yields. In striking contrast, *p*-(trifluoromethyl)benzaldehyde (**3g**) and *p*-formylacetophenone (**3h**) showed extremely low conversions, affording hardly any of the corresponding adducts, and therefore evidencing the inefficiency of electron-deficient formyl groups. It is assumed that an electron-deficient formyl group has weak coordination ability, resulting in an inefficient conversion. In contrast, the reaction of 2-formylthiophene (**3i**) reached completion within 5 h, affording the corresponding product **4fi** in 69% yield. In addition to (hetero)arylaldehydes, *p*-methoxycinnamaldehyde (**3j**) also participated in the reaction, producing **4fj** in 81% yield. However, no reaction occurred when 3-phenylpropanal, *p*-methoxyacetophenone, or ethyl pyruvate were used. Thus, we confirmed that α,β -unsaturated aldehydes are essential as carbonyl components.



Scheme 6. Reactions of diyne **2f** with various aldehydes and ketones.

Hydrocarbamoylative cyclization of 1,6-diynes bearing tertiary or quaternary carbon tethers with DMF. In our previous study, hydrocarbamoylative cyclization of diyne **2m** bearing a malonate tether with DMF was very sluggish, even at 140 °C, and the yield of **6m** was as low as 30% (Scheme 7a).⁸ Based on the follow-up computational study, it is assumed that hydrocarbamoylative cyclization proceeds via

(1) oxidative coupling of diyne **2m** with Cp***RuH** species, which is assumed to be generated from Cp***Ru**⁺ with Me₂NH, and subsequent reductive elimination from the resultant ruthenacycle **7**, (2) insertion of DMF into the Ru–C bond of **8**, and (3) β-H elimination from alkoxoruthenium **9** (Scheme 7b).¹² In this proposed mechanism, the final step was considered to be the most problematic owing to the steric repulsion between the bulky Cp* ligand and the methoxycarbonyl substituent in **TS_{9-6m}**. Our investigation examining the reactions of 1,6-diyne with aldehydes showed that complex **1b** with a smaller Cp ligand is superior to the bulkier Cp* complex **1a** when bulky diynes equipped with *tert*-butyl terminal groups were used as substrates. For this reason, it was presumed that the smaller catalyst **1b** is more suitable than **1a** for the challenging hydrocarbonylative cyclization of bulky diynes.

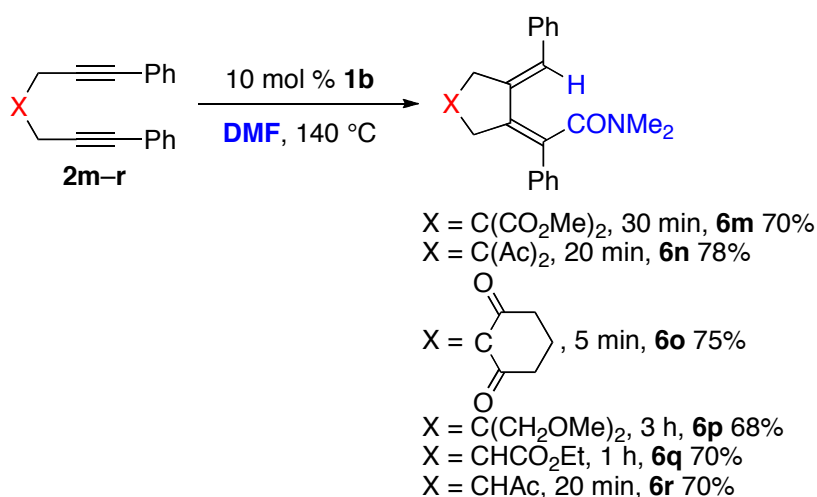


Scheme 7. (a) Previous hydrocarbamoylative cyclization of diyne **2m** with DMF and

(b) a proposed mechanism for this process.

Thus, the reactions of diynes bearing tertiary or quaternary carbon tethers with DMF were briefly revisited using catalyst **1b** (Scheme 8). Gratifyingly, the reaction of diyne **2m** was completed within 30 min in the presence of 10 mol % **1b** at 140 °C, affording **6m** in 70% yield. Similarly, acetylacetonone derivative **6n** and cyclohexane-1,3-dione derivative **6o** were obtained in 78% and 75% yields, respectively.

The reaction of **2p** without a carbonyl group also afforded **6p** in 68% yield, even though a longer reaction time of 3 h was required. Moreover, diynes **2q** and **2r** bearing tertiary carbon tethers were converted into the corresponding products in 70% yield. These new results are markedly superior to those previously obtained with the bulkier catalyst **1a**.



Scheme 8. Hydrocarbomylative cyclization of diynes **2m–r** using catalyst **1b**.

Conclusion

We have demonstrated that the ruthenium-catalyzed reaction of diynes bearing alkyl terminal groups with arylaldehydes afforded diene ketones with a stereoselectivity that was significantly different from that of the previously reported

rhodium-catalyzed reactions. The results of DFT calculations suggest that this characteristic stereoselectivity could be attributed to the direct ring opening of the initially formed ruthenium η^4 -pyran complex. Although the dienyne ketone products could undergo isomerization under the reaction conditions, thereby decreasing the stereoselectivity, the reactions of diynes bearing bulky *tert*-butyl terminal groups using $[\text{CpRu}(\text{MeCN})_3]\text{PF}_6$ as the catalyst produced the (*Z*)-products as the exclusive stereoisomer. A variety of arylaldehydes with alkyl, alkoxy, and halogen substituents, 2-thienylaldehyde, as well as cinnamaldehyde successfully reacted. Nevertheless, strong electron-withdrawing groups on arylaldehydes were found to be detrimental to the reaction. Likewise, no reaction occurred when saturated aldehyde and ketones were employed, thus demonstrating that α,β -unsaturated aldehydes are key reaction components. Challenging hydrocarbonylative cyclization of diynes bearing tertiary or quaternary carbon tethers was also successful when smaller $[\text{CpRu}(\text{MeCN})_3]\text{PF}_6$ was employed as the catalyst.

Experimental Section

General. Column chromatography was performed on silica gel (Cica silica gel 60N) with solvents specified below. ^1H and ^{13}C NMR spectra were obtained for samples in CDCl_3 solutions at 25 °C. ^1H NMR chemical shifts are reported in terms of chemical shift (δ , ppm) relative to the singlet at δ 7.26 ppm for chloroform. Splitting patterns are designated as follows: s, singlet; d, doublet; t, triplet; q, quartet; quint, quintet; sext, sextet; sept, septet; m, multiplet. Coupling constants are reported in Hz. ^{13}C NMR spectra were fully decoupled and are reported in terms of chemical shift (δ , ppm) relative to the triplet at δ 77.0 ppm for CDCl_3 . High resolution mass spectra (HRMS) were obtained on a ESI- or DART-TOF mass spectrometer. Aldehydes, ketones, and dry solvents were purchased and used as received. 1,6-Diynes **2a**, **2b**, **2c**, **2g**, **2i**, and **2l-r** were known compounds.^{8,11,13} Ruthenium catalysts **1a** and **1b** were prepared according to the literature procedures.¹⁴

Preparation of 1,6-Diynes

General procedure for *N,N*-Dipropargylsulfonamides – Synthesis of *N,N*-bis(4,4-dimethylpent-2-ynyl)-4-methylbenzenesulfonamide (2f**):** To a solution of TsNH_2 (172.2 mg, 1.01 mmol) in DMF (2 mL) was added NaH (ca. 60 wt% in

mineral oil, 90.0 mg, 2.25 mmol) at 0 °C. The mixture was stirred at 0 °C for 15 min and at room temperature for 1 h. To this mixture was added a preformed solution of 4,4-dimethylpent-2-ynyl methanesulfonate (433.9 mg, 2.28 mmol) in dry DMF (4 mL) at room temperature. The reaction mixture was stirred at room temperature for 2 h. The reaction was quenched with sat. NH₄Cl (5 mL). The aqueous phase was extracted with AcOEt/hexane (5:1, 3 × 5 mL). The combined organic layer was washed with brine (3 × 10 mL), and dried over MgSO₄. After concentration *in vacuo*, the obtained crude product was purified by silica gel chromatography (hexane/AcOEt = 10:1) to afford diyne **2f** (182.1 mg, 50% yield) as a white solid (mp 105.9–107.3 °C); ¹H NMR (400 MHz, CDCl₃, 25 °C) δ 1.06 (s, 18 H), 2.41 (s, 3 H), 4.10 (s, 4 H), 7.28 (d, *J* = 8.0 Hz, 2 H), 7.70 (d, *J* = 8.0 Hz, 2 H); ¹³C NMR (100 MHz, CDCl₃, 25 °C) δ 21.4, 27.2, 30.7, 36.5, 70.8, 94.3, 127.8, 129.5, 135.7, 143.4; HRMS (ESI) *m/z* calcd for C₂₁H₂₉NO₂S•Na 382.1817, found 382.1817 [M+Na]⁺.

Analytical data for *N,N*-di(hex-2-ynyl)-4-methylbenzenesulfonamide (2d):

146.9 mg, 38%; yellow oil; ¹H NMR (400 MHz, CDCl₃, 25 °C) δ 0.86 (t, *J* = 7.2 Hz, 6 H), 1.36 (sext, *J* = 7.2 Hz, 4 H), 1.98 (tt, *J* = 7.2, 2.2 Hz, 4 H), 2.40 (s, 3 H), 4.10 (t, *J*

= 2.2 Hz, 4 H), 7.26 (d, $J = 8.4$ Hz, 2 H), 7.70 (d, $J = 8.4$ Hz, 2 H); ^{13}C NMR (100 MHz, CDCl_3 , 25 °C) δ 13.3, 20.5, 21.4, 21.8, 36.6, 72.5, 86.0, 127.9, 129.2, 135.6, 143.3; HRMS (ESI) m/z calcd for $\text{C}_{19}\text{H}_{25}\text{NO}_2\text{S}\cdot\text{Na}$ 354.1504, found 354.1509 $[\text{M}+\text{Na}]^+$.

Analytical data for

4-methyl-*N,N*-bis(4-methylpent-2-ynyl)benzenesulfonamide (2e): 58.1 mg, 19%; white solid (mp 97.1–98.6 °C); ^1H NMR (400 MHz, CDCl_3 , 25 °C) δ 1.10 (d, $J = 7.2$ Hz, 12 H), 2.34–2.42 (m, 2 H), 2.40 (s, 3 H), 4.10 (d, $J = 2.0$ Hz, 4 H), 7.28 (d, $J = 8.0$ Hz, 2 H), 7.71 (d, $J = 8.0$ Hz, 2 H); ^{13}C NMR (100 MHz, CDCl_3 , 25 °C) δ 20.3, 21.4, 22.6, 36.5, 71.6, 91.5, 127.9, 129.4, 135.8, 143.4; HRMS (ESI) m/z calcd for $\text{C}_{19}\text{H}_{25}\text{NO}_2\text{S}\cdot\text{Na}$ 354.1504, found 354.1502 $[\text{M}+\text{Na}]^+$.

Synthesis of 1-(4,4-dimethylpent-2-ynyloxy)-4,4-dimethylpent-2-yne (2h):

To a suspension of NaH (ca. 60 wt% in mineral oil, 68.0 mg, 1.6 mmol) in dry MeCN (6 mL) was added a 4,4-dimethylpent-2-yn-1-ol (113.8 mg, 1.01 mmol) at 0 °C and the mixture was stirred at room temperature for 1 h. To this mixture was added a preformed solution of 4,4-dimethylpent-2-ynyl methanesulfonate (231.8 mg, 1.22 mmol). The

reaction mixture was stirred at room temperature for 2.5 h. The reaction was quenched with sat. NH_4Cl (5 mL). The aqueous phase was extracted with Et_2O (3×5 mL). The combined organic layer was washed with brine (3×10 mL), and dried over MgSO_4 . After concentration *in vacuo*, the obtained crude product was purified by silica gel chromatography (hexane/ AcOEt = 5:1) to afford diyne **2h** (103.0 mg, 50% yield) as an orange oil; ^1H NMR (400 MHz, CDCl_3 , 25 °C) δ 1.22 (s, 18 H), 4.19 (s, 4 H); ^{13}C NMR (100 MHz, CDCl_3 , 25 °C) δ 27.4, 30.9, 56.9, 73.8, 95.5; HRMS (ESI) m/z calcd for $\text{C}_{14}\text{H}_{22}\text{O}\cdot\text{Na}$ 229.1568, found 229.1574 $[\text{M}+\text{Na}]^+$.

Synthesis of 3,3-bis(4,4-dimethylpent-2-ynyl)pentane-2,4-dione (2j): To a solution of acetylacetone (500.7 mg, 5.00 mmol) and 4,4-dimethylpent-2-ynyl methanesulfonate (1.950 g, 10.3 mmol) in dry MeCN (20 mL) was added K_2CO_3 (4.181 g, 30.3 mmol) at room temperature. The resultant mixture was stirred at 60 °C for 18.5 h. The reaction was quenched with H_2O (20 mL). The aqueous phase was extracted with Et_2O (20 mL). The organic layer was washed with H_2O (3×10 mL), brine (20 mL), and dried over MgSO_4 . After concentration *in vacuo*, the obtained crude product was purified by silica gel chromatography (hexane/ AcOEt = 10:1) to afford diyne **2j** (1.086

g, 75% yield) as a pale-yellow solid (mp 102.6–104.1 °C); ¹H NMR (400 MHz, CDCl₃, 25 °C) δ 1.15 (s, 18 H), 2.15 (s, 6 H), 2.85 (s, 4 H); ¹³C NMR (100 MHz, CDCl₃, 25 °C) δ 21.3, 26.6, 27.3, 31.0, 70.9, 73.4, 92.6, 203.7; IR (neat) 1697 (C=O) cm⁻¹; HRMS (ESI) *m/z* calcd for C₁₉H₂₈O₂•Na 311.1987, found 311.1982 [M+Na]⁺.

Synthesis of 2,2-bis(4,4-dimethylpent-2-ynyl)malononitrile (2k): To a solution of 4,4-dimethylpent-2-ynyl methanesulfonate (1.998 g, 10.5 mmol), Et₃N (1.48 mL, 10.6 mmol), and NaI (1.724 g, 11.5 mmol) in DMSO (15 mL) was added malononitrile (330.6 mg, 5.00 mmol) at 0 °C. The resultant mixture was stirred at 50 °C for 16 h. The reaction was quenched with H₂O (20 mL). The aqueous phase was extracted with AcOEt (20 mL). The organic layer was washed with H₂O (3 × 20 mL), brine (20 mL), and dried over MgSO₄. After concentration *in vacuo*, the obtained crude product was purified by silica gel chromatography (hexane/AcOEt = 10:1) to afford diyne **2k** (200.4 mg, 16% yield) as a yellow paste; ¹H NMR (400 MHz, CDCl₃, 25 °C) δ 1.24 (s, 18 H), 2.93 (s, 4 H); ¹³C NMR (100 MHz, CDCl₃, 25 °C) δ 27.5, 27.8, 30.7, 37.6, 69.0, 96.3, 114.3; IR (neat) 2245 (C≡N) cm⁻¹; HRMS (ESI) *m/z* calcd for C₁₇H₂₂N₂•Na 277.1681, found 277.1687 [M+Na]⁺.

Reaction of Diynes with Aldehydes.

General procedure 1 – Synthesis of

(4-(2-(4-methoxyphenyl)-1-phenylvinyl)-2,5-dihydrofuran-3-yl)(phenyl)methanone

(4aa): A solution of diyne **2a** (74.1 mg, 0.301 mmol), aldehyde **3a** (110 μ L, 0.90 mmol), and catalyst **1a** (15.1 mg, 0.030 mmol) in dry THF (1.0 mL) was degassed at -78 $^{\circ}$ C and backfilled with argon (three times). The reaction mixture was stirred at 70 $^{\circ}$ C for 20 min. After concentration in *vacuo*, the crude product was purified by flash column chromatography on silica gel (hexane/AcOEt, 10:1) to afford **4aa** (90.9 mg, 79%) as a yellow paste: ^1H NMR (400 MHz, CDCl_3 , 25 $^{\circ}$ C) *Z* isomer δ 3.85 (s, 3 H), 4.90 (t, $J = 4.6$ Hz, 2 H), 5.16 (t, $J = 4.6$ Hz, 2 H), 6.54 (d, $J = 8.8$ Hz, 2 H), 6.61 (s, 1 H), 6.68 (d, $J = 8.8$ Hz, 2 H), 6.85–7.62 (m, 10 H); *E* isomer δ 3.68 (s, 3 H), 5.05–5.11 (m, 4 H), 6.44 (s, 1 H), 6.92 (d, $J = 8.8$ Hz, 2 H), 7.33 (d, $J = 8.8$ Hz, 2 H), 6.85–7.62 (m, 10 H); ^{13}C NMR (100 MHz, CDCl_3 , 25 $^{\circ}$ C) *E* + *Z* δ 55.1, 55.3, 78.1, 78.3, 79.3, 113.3, 114.2, 126.3, 127.3, 127.5, 127.7, 128.0, 128.1, 128.26, 128.31, 128.4, 128.7, 129.0, 129.9, 130.2, 130.6, 130.8, 131.5, 132.0, 132.2, 132.5, 132.8, 134.0, 136.8, 137.1, 138.0, 138.1, 141.2, 143.1, 147.6, 159.0, 159.4, 192.4, 194.1; IR (neat) 1645 (C=O)

cm⁻¹; HRMS (ESI) *m/z* calcd for C₂₆H₂₂O₃•Na 405.1467, found 405.1465 [M+Na]⁺.

Analytical data for dimethyl

3-acetyl-4-(1-(4-methoxyphenyl)prop-1-en-2-yl)cyclopent-3-ene-1,1-dicarboxylate

(4ba):^{5b} The reaction was performed at room temperature, 98.7 mg, 88%; yellow oil; ¹H NMR (400 MHz, CDCl₃, 25 °C) *Z* isomer δ 2.04 (s, 3 H), 2.21 (s, 3 H), 3.29 (s, 2 H), 3.36 (s, 2 H), 3.72 (s, 6 H), 3.77 (s, 3 H), 6.33 (s, 1 H), 6.78 (d, *J* = 8.8 Hz, 2 H), 7.13 (d, *J* = 8.8 Hz, 2 H); *E* isomer δ 2.04 (s, 3 H), 2.25 (s, 3 H), 3.37 (s, 4 H), 3.75 (s, 6 H), 3.81 (s, 3 H), 6.37 (s, 1 H), 6.89 (d, *J* = 8.4 Hz, 2 H), 7.24 (d, *J* = 8.4 Hz, 2 H); ¹³C NMR (100 MHz, CDCl₃, 25 °C) *Z* isomer δ 24.6, 28.0, 41.3, 45.0, 53.1, 55.2, 56.1, 113.9, 127.9, 128.9, 130.3, 130.6, 135.5, 152.2, 158.7, 171.7, 196.3; IR (neat) 1736 (C=O), 1657 (C=O) cm⁻¹.

Analytical data for

1-(4-(1-(4-methoxyphenyl)prop-1-en-2-yl)-1-tosyl-2,5-dihydro-1H-pyrrol-3-yl)ethanone (4ca):

The reaction was performed at room temperature and the product was isolated by recrystallization from CH₂Cl₂/hexane., 95.1 mg, 77%; white solid (mp 138.1–139.4 °C); *Z* isomer; ¹H NMR (400 MHz, CDCl₃, 25 °C) δ 1.99 (d, *J* = 1.2

Hz, 3 H), 2.16 (s, 3 H), 2.47 (s, 3 H), 3.79 (s, 3 H), 4.33–4.37 (m, 4 H), 6.37 (s, 1 H), 6.63 (d, $J = 8.8$ Hz, 2 H), 6.93 (d, $J = 8.8$ Hz, 2 H), 7.35 (d, $J = 8.0$ Hz, 2 H), 7.72 (d, $J = 8.0$ Hz, 2 H); ^{13}C NMR (100 MHz, CDCl_3 , 25 °C) δ 21.5, 24.5, 27.9, 55.2, 55.5, 58.0, 114.1, 127.0, 127.7, 128.2, 128.8, 129.88, 129.94, 133.2, 133.3, 143.9, 148.9, 159.0, 194.4; IR (neat) 1660 (C=O) cm^{-1} ; HRMS (DART) m/z calcd for $\text{C}_{27}\text{H}_{33}\text{NO}_4\text{S}\cdot\text{NH}_4$ 429.1848, found 429.1855 $[\text{M}+\text{NH}_4]^+$.

Analytical data for

1-(4-(1-(4-methoxyphenyl)pent-1-en-2-yl)-1-tosyl-2,5-dihydro-1H-pyrrol-3-yl)butan

-1-one (4da): 124.7 mg, 86%; brown oil; *Z* isomer; ^1H NMR (400 MHz, CDCl_3 , 25 °C) δ 0.76 (t, $J = 7.2$ Hz, 3 H), 0.93 (t, $J = 7.2$ Hz, 3 H), 1.30–1.50 (m, 4 H), 2.21 (t, $J = 7.6$ Hz, 2 H), 2.44 (t, $J = 7.6$ Hz, 2 H), 2.47 (s, 3 H), 3.79 (s, 3 H), 4.25–4.41 (m, 4 H), 6.34 (s, 1 H), 6.62 (d, $J = 8.4$ Hz, 2 H), 6.95 (d, $J = 8.4$ Hz, 2 H), 7.34 (d, $J = 8.4$ Hz, 2 H), 7.71 (d, $J = 8.4$ Hz, 2 H); ^{13}C NMR (100 MHz, CDCl_3 , 25 °C) δ 13.6, 13.8, 16.8, 21.4, 21.5, 40.7, 42.1, 55.2, 55.7, 58.6, 114.0, 127.6, 128.5, 128.8, 128.9, 129.4, 129.9, 131.9, 133.3, 133.4, 143.8, 147.3, 158.8, 197.1; IR (neat) 1660 (C=O) cm^{-1} ; HRMS (ESI) m/z calcd for $\text{C}_{27}\text{H}_{33}\text{NO}_4\text{S}\cdot\text{Na}$ 490.2028, found 490.2013 $[\text{M}+\text{Na}]^+$.

Analytical data for
1-(4-(1-(4-methoxyphenyl)-3-methylbut-1-en-2-yl)-1-tosyl-2,5-dihydro-1H-pyrrol-3-yl)-2-methylpropan-1-one (4ea): 107.4 mg, 82%; white solid (mp 119.0–120.2 °C); *Z* isomer; ¹H NMR (400 MHz, CDCl₃, 25 °C) δ 0.86 (d, *J* = 6.8 Hz, 6 H), 1.06 (d, *J* = 6.8 Hz, 6 H), 2.36 (sept, *J* = 6.8 Hz, 1 H), 2.46 (s, 3 H), 3.02 (sept, *J* = 6.8 Hz, 1 H), 3.79 (s, 3 H), 4.26 (t, *J* = 4.2 Hz, 2 H), 4.38 (t, *J* = 4.2 Hz, 2 H), 6.32 (s, 1 H), 6.63 (d, *J* = 8.6 Hz, 2 H), 6.96 (d, *J* = 8.6 Hz, 2 H), 7.34 (d, *J* = 8.2 Hz, 2 H), 7.70 (d, *J* = 8.2 Hz, 2 H); ¹³C NMR (100 MHz, CDCl₃, 25 °C) δ 15.2, 18.4, 21.5, 21.8, 35.8, 37.4, 55.2, 55.9, 58.8, 65.8, 113.9, 126.5, 127.6, 128.6, 129.2, 129.9, 132.9, 138.0, 143.8, 147.2, 158.8, 202.0; IR (neat) 1660 (C=O) cm⁻¹; HRMS (ESI) *m/z* calcd for C₂₇H₃₃NO₄S•Na 490.2028, found 490.2039 [M+Na]⁺.

General procedure 2 – Synthesis of
(Z)-1-(4-(1-(4-methoxyphenyl)-3,3-dimethylbut-1-en-2-yl)-1-tosyl-2,5-dihydro-1H-pyrrol-3-yl)-2,2-dimethylpropan-1-one (4fa): A solution of diyne **2f** (108.6 mg, 0.302 mmol), aldehyde **3a** (110 μL, 0.90 mmol), and catalyst **1b** (13.2 mg, 0.030 mmol) in dry THF (1.0 mL) was degassed at –78 °C and backfilled with argon (three times).

The reaction mixture was stirred at 70 °C for 10 h. After concentration in vacuo, the crude product was purified by flash column chromatography on silica gel (hexane/AcOEt, 10:1) to afford **4fa** (127.9 mg, 85%) as a pale-yellow solid (mp 120.6–122.1 °C): ¹H NMR (400 MHz, CDCl₃, 25 °C) δ 0.94 (s, 9 H), 1.07 (s, 9 H), 2.48 (s, 3 H), 3.77 (s, 3 H), 4.00 (ddd, *J* = 15.6, 6.0, 3.2 Hz, 1 H), 4.20 (ddd, *J* = 15.6, 5.4, 2.8 Hz, 1 H), 4.40 (ddd, *J* = 13.2, 5.4, 3.2 Hz, 1 H), 4.56 (ddd, *J* = 13.2, 6.0, 2.8 Hz, 1 H), 6.34 (s, 1 H), 6.57 (d, *J* = 8.6 Hz, 2 H), 6.95 (d, *J* = 8.6 Hz, 2 H), 7.34 (d, *J* = 8.0 Hz, 2 H), 7.68 (d, *J* = 8.0 Hz, 2 H); ¹³C NMR (100 MHz, CDCl₃, 25 °C) δ 21.5, 25.9, 30.3, 36.5, 43.8, 55.1, 55.9, 57.9, 113.6, 125.5, 127.5, 129.2, 129.7, 129.9, 132.8, 133.3, 141.8, 143.9, 146.0, 158.3, 202.9; IR (neat) 1680 (C=O) cm⁻¹; HRMS (ESI) *m/z* calcd for C₂₉H₃₇NO₄S•Na 518.2341, found 518.2347 [M+Na]⁺.

Analytical data for (Z)-1-(4-(1-(4-methoxyphenyl)-3,3-dimethylbut-1-en-2-yl)-2,5-dihydrofuran-3-yl)-2,2-dimethylpropan-1-one (4ha): 90.2 mg, 85%; dark-brown oil; ¹H NMR (400 MHz, CDCl₃, 25 °C) δ 0.98 (s, 9 H), 1.17 (s, 9 H), 3.78 (s, 3 H), 4.52 (dt, *J* = 14.0, 4.8 Hz, 1 H), 4.69 (dt, *J* = 14.0, 4.8 Hz, 1 H), 4.95–5.07 (m, 2 H), 6.41 (s, 1 H), 6.79 (d, *J* =

8.8 Hz, 2 H), 7.19 (d, $J = 8.8$ Hz, 2 H); ^{13}C NMR (100 MHz, CDCl_3 , 25 °C) δ 25.7, 30.4, 36.5, 43.8, 55.2, 76.2, 78.1, 113.6, 125.0, 129.4, 130.2, 134.6, 141.5, 148.6, 158.3, 203.1; IR (neat) 1643 (C=O) cm^{-1} ; HRMS (ESI) m/z calcd for $\text{C}_{22}\text{H}_{30}\text{O}_3\cdot\text{Na}$ 365.2093, found 365.2072 $[\text{M}+\text{Na}]^+$.

Analytical data for (Z)-dimethyl

3-(1-(4-methoxyphenyl)-3,3-dimethylbut-1-en-2-yl)-4-pivaloylcyclopent-3-ene-1,1-di

carboxylate (4ia): This compound was isolated after the treatment of a crude product

with $\text{NaBH}[\text{OCH}(\text{CF}_3)_2]_3$ (7.0 equiv) in $(\text{CF}_3)_2\text{CHOH}$; 111.2 mg, 81%; yellow oil;

^1H NMR (400 MHz, CDCl_3 , 25 °C) δ 1.03 (s, 9 H), 1.15 (s, 9 H), 3.00 (dt, $J = 18.0$, 1.8

Hz, 1 H), 3.31 (dt, $J = 18.0$, 1.8 Hz, 1 H), 3.37 (dt, $J = 16.0$, 1.8 Hz, 1 H), 3.55 (dt, $J =$

16.0, 1.8 Hz, 1 H), 3.69 (s, 3 H), 3.756 (s, 3 H), 3.761 (s, 3 H), 6.32 (s, 1 H), 6.75 (d, J

= 8.4 Hz, 2 H), 7.11 (d, $J = 8.4$ Hz, 2 H); ^{13}C NMR (100 MHz, CDCl_3 , 25 °C) δ 26.3,

30.5, 36.7, 42.7, 43.7, 45.6, 53.0, 53.1, 55.2, 58.3, 113.5, 123.9, 129.4, 130.4, 135.6,

145.1, 148.7, 158.1, 171.5, 171.9, 205.2; IR (neat) 1738 (C=O), 1676 (C=O) cm^{-1} ;

HRMS (ESI) m/z calcd for $\text{C}_{27}\text{H}_{36}\text{O}_6\cdot\text{Na}$ 479.2410, found 479.2402 $[\text{M}+\text{Na}]^+$.

Analytical data for

(Z)-1,1'-(3-(1-(4-methoxyphenyl)-3,3-dimethylbut-1-en-2-yl)-4-pivaloylcyclopent-3-ene-1,1-diyl)diethanone (4ja): 102.2 mg, 80%; yellow oil; ¹H NMR (400 MHz, CDCl₃, 25 °C) δ 1.09 (s, 9 H), 1.12 (s, 9 H), 1.89 (s, 3 H), 2.13 (s, 3 H), 2.72 (d, *J* = 18.4 Hz, 1 H), 3.16 (d, *J* = 16.0 Hz, 1 H), 3.24 (d, *J* = 18.4 Hz, 1 H), 3.54 (d, *J* = 16.0 Hz, 1 H), 3.76 (s, 3 H), 6.33 (s, 1 H), 6.73 (d, *J* = 8.8 Hz, 2 H), 7.14 (d, *J* = 8.8 Hz, 2 H); ¹³C NMR (100 MHz, CDCl₃, 25 °C) δ 26.0, 26.3, 26.4, 30.5, 36.7, 39.5, 42.6, 43.8, 55.2, 72.9, 113.6, 124.0, 129.3, 130.4, 135.8, 145.2, 148.1, 158.3, 203.6, 203.7, 205.7; IR (neat) 1701 (C=O), 1674 (C=O) cm⁻¹; HRMS (ESI) *m/z* calcd for C₂₇H₃₆O₄•Na 447.2511, found 447.2529 [M+Na]⁺.

Analytical data for

(Z)-3-(1-(4-methoxyphenyl)-3,3-dimethylbut-1-en-2-yl)-4-pivaloylcyclopent-3-ene-1,1-dicarbonitrile (4ka): 174.4 mg, 58%; yellow oil; ¹H NMR (400 MHz, CDCl₃, 25 °C) δ 1.04 (s, 9 H), 1.18 (s, 9 H), 3.13 (dt, *J* = 17.6, 1.6 Hz, 1 H), 3.26 (dt, *J* = 17.6, 1.4 Hz, 1 H), 3.49 (dt, *J* = 16.0, 1.6 Hz, 1 H), 3.63 (d, *J* = 16.0, 1.6 Hz, 1 H), 3.78 (s, 3 H), 6.46 (s, 1 H), 6.82 (d, *J* = 8.8 Hz, 2 H), 7.21 (d, *J* = 8.8 Hz, 2 H); ¹³C NMR (100 MHz, CDCl₃, 25 °C) δ 26.2, 30.5, 31.5, 37.2, 44.0, 46.4, 48.4, 55.3, 114.0, 115.7, 116.1,

126.0, 129.3, 129.6, 134.7, 142.7, 147.1, 158.8, 203.9; IR (neat) 2362 (C≡N), 1680 (C=O) cm⁻¹; HRMS (ESI) *m/z* calcd for C₂₅H₃₀N₂O₂•Na 413.2205, found 413.2202 [M+Na]⁺.

Analytical data for (Z)-dimethyl 3-acetyl-4-(1-(4-methoxyphenyl)-3,3-dimethylbut-1-en-2-yl)cyclopent-3-ene-1,1-dicarboxylate (4la): 54.0 mg, 43%; pale-yellow oil; ¹H NMR (400 MHz, CDCl₃, 25 °C) δ 1.21 (s, 9 H), 2.15 (s, 3 H), 3.17 (d, *J* = 19.0 Hz, 1 H), 3.30 (d, *J* = 17.2 Hz, 1 H), 3.45 (d, *J* = 17.2 Hz, 1 H), 3.60 (d, *J* = 19.0 Hz, 1 H), 3.71 (s, 3 H), 3.75 (s, 3 H), 3.77 (s, 3 H), 6.47 (s, 1 H), 6.78 (d, *J* = 8.6 Hz, 2 H), 7.14 (d, *J* = 8.6 Hz, 2 H); ¹³C NMR (100 MHz, CDCl₃, 25 °C) δ 28.5, 30.9, 36.8, 41.5, 47.8, 52.98, 53.04, 55.2, 56.1, 113.9, 125.8, 129.25, 129.34, 137.3, 143.7, 149.6, 158.6, 171.7, 172.0, 197.1; IR (neat) 1736 (C=O), 1658 (C=O) cm⁻¹; HRMS (DART) *m/z* calcd for C₂₄H₃₀O₆•H 415.2121, found 415.2118 [M+H]⁺.

Analytical data for (Z)-1-(4-(1-(2-methoxyphenyl)-3,3-dimethylbut-1-en-2-yl)-1-tosyl-2,5-dihydro-1H-pyrrol-3-yl)-2,2-dimethylpropan-1-one (4fb): 126.9 mg, 85%; white solid (mp.

121.3–122.8 °C); ¹H NMR (400 MHz, CDCl₃, 25 °C) δ 0.88 (s, 9 H), 1.09 (s, 9 H), 2.46 (s, 3 H), 3.76 (s, 3 H), 3.95 (ddd, *J* = 15.6, 5.4, 3.8 Hz, 1 H), 4.21 (ddd, *J* = 15.6, 5.6, 2.8 Hz, 1 H), 4.34 (ddd, *J* = 13.2, 5.6, 3.2 Hz, 1 H), 4.47 (ddd, *J* = 13.2, 6.0, 2.8 Hz, 1 H), 6.51 (t, *J* = 7.4 Hz, 1 H), 6.54 (s, 1 H), 6.75 (d, *J* = 7.6 Hz, 1 H), 6.94 (dd, *J* = 7.6, 1.6 Hz, 1 H), 7.07 (dt, *J* = 8.0, 1.6 Hz, 1 H), 7.31 (d, *J* = 8.0 Hz, 2 H), 7.64 (d, *J* = 8.0 Hz, 2 H); ¹³C NMR (100 MHz, CDCl₃, 25 °C) δ 21.5, 25.8, 30.3, 36.6, 43.6, 55.4, 55.8, 58.2, 110.3, 120.2, 121.9, 126.3, 127.4, 128.1, 128.5, 129.9, 132.7, 133.3, 143.3, 143.7, 146.3, 157.0, 202.9; IR (neat) 1680 (C=O) cm⁻¹; HRMS (ESI) *m/z* calcd for C₂₉H₃₇NO₄S•Na 518.2341, found 518.2349 [M+Na]⁺.

Analytical data for

(*Z*)-1-(4-(3,3-dimethyl-1-*p*-tolylbut-1-en-2-yl)-1-tosyl-2,5-dihydro-1*H*-pyrrol-3-yl)-2,

2-dimethylpropan-1-one (4fc): 117.6 mg, 82%; white solid (mp. 102.8–104.5 °C);

¹H NMR (400 MHz, CDCl₃, 25 °C) δ 0.89 (s, 9 H), 1.08 (s, 9 H), 2.26 (s, 3 H), 2.48 (s, 3 H), 4.05 (ddd, *J* = 15.6, 5.8, 3.4 Hz, 1 H), 4.23 (ddd, *J* = 15.6, 5.8, 3.0 Hz, 1 H), 4.42 (ddd, *J* = 13.2, 5.6, 3.6 Hz, 1 H), 4.53 (ddd, *J* = 13.2, 6.0, 2.8 Hz, 1 H), 6.35 (s, 1 H), 6.83 (d, *J* = 8.0 Hz, 2 H), 6.88 (d, *J* = 8.0 Hz, 2 H), 7.35 (d, *J* = 8.0 Hz, 2 H), 7.71 (d, *J*

= 8.0 Hz, 2 H); ^{13}C NMR (100 MHz, CDCl_3 , 25 °C) δ 21.1, 21.6, 25.8, 30.3, 36.4, 43.8, 55.8, 58.0, 126.0, 127.5, 127.9, 128.8, 129.9, 132.7, 133.3, 134.2, 136.2, 142.9, 143.8, 146.1, 202.6; IR (neat) 1680 (C=O) cm^{-1} ; HRMS (ESI) m/z calcd for $\text{C}_{29}\text{H}_{37}\text{NO}_3\text{S}\cdot\text{Na}$ 502.2392, found 502.2395 $[\text{M}+\text{Na}]^+$.

Analytical data for
(Z)-1-(4-(1-(4-fluorophenyl)-3,3-dimethylbut-1-en-2-yl)-1-tosyl-2,5-dihydro-1H-pyrrol-3-yl)-2,2-dimethylpropan-1-one (4fd): 125.9 mg, 84%; white solid (mp. 114.6–116.3 °C); ^1H NMR (400 MHz, CDCl_3 , 25 °C) δ 0.99 (s, 9 H), 1.08 (s, 9 H), 2.48 (s, 3 H), 3.80 (ddd, $J = 15.6, 5.6, 3.6$ Hz, 1 H), 4.17 (ddd, $J = 15.6, 6.0, 2.6$ Hz, 1 H), 4.31 (ddd, $J = 13.4, 5.2, 3.6$ Hz, 1 H), 4.62 (ddd, $J = 13.4, 6.0, 2.8$ Hz, 1 H), 6.36 (s, 1 H), 6.66 (t, $J = 8.8$ Hz, 2 H), 6.98 (dd, $J = 8.8, 5.6$ Hz, 2 H), 7.32 (d, $J = 8.0$ Hz, 2 H), 7.61 (d, $J = 8.0$ Hz, 2 H); ^{13}C NMR (100 MHz, CDCl_3 , 25 °C) δ 21.5, 25.9, 30.2, 36.7, 43.8, 55.8, 57.7, 114.9 (d, $J = 21.0$ Hz), 124.8, 127.4, 129.4 (d, $J = 7.6$ Hz), 130.0, 132.9, 133.2 (2C), 143.7, 144.1, 145.8, 161.5 (d, $J = 245.1$ Hz), 203.0; IR (neat) 1680 (C=O) cm^{-1} ; HRMS (ESI) m/z calcd for $\text{C}_{28}\text{H}_{34}\text{FNO}_3\text{S}\cdot\text{Na}$ 506.2141, found 506.2115 $[\text{M}+\text{Na}]^+$.

Analytical data for

(Z)-1-(4-(1-(4-chlorophenyl)-3,3-dimethylbut-1-en-2-yl)-1-tosyl-2,5-dihydro-1H-pyrrol-3-yl)-2,2-dimethylpropan-1-one (4fe): 120.8 mg, 81%; white solid (mp. 134.5–135.9 °C); ¹H NMR (400 MHz, CDCl₃, 25 °C) δ 0.97 (s, 9 H), 1.08 (s, 9 H), 2.50 (s, 3 H), 3.88 (ddd, *J* = 15.6, 6.0, 3.6 Hz, 1 H), 4.21 (ddd, *J* = 15.6, 5.6, 2.4 Hz, 1 H), 4.33 (ddd, *J* = 13.2, 6.0, 3.6 Hz, 1 H), 4.62 (ddd, *J* = 13.2, 6.0, 2.4 Hz, 1 H), 6.34 (s, 1 H), 6.92 (d, *J* = 9.6 Hz, 2 H), 6.95 (d, *J* = 9.6 Hz, 2 H), 7.35 (d, *J* = 8.4 Hz, 2 H), 7.64 (d, *J* = 8.4 Hz, 2 H); ¹³C NMR (100 MHz, CDCl₃, 25 °C) δ 21.6, 25.8, 30.2, 36.8, 43.8, 55.7, 57.7, 124.7, 127.4, 128.2, 129.1, 130.0, 132.3, 133.0, 133.2, 135.6, 144.1, 144.5, 145.8, 202.7; IR (neat) 1680 (C=O) cm⁻¹; HRMS (ESI) *m/z* calcd for C₂₈H₃₄ClNO₃S•Na 522.1846, found 522.1824 [M+Na]⁺.

Analytical data for

(Z)-1-(4-(1-(4-bromophenyl)-3,3-dimethylbut-1-en-2-yl)-1-tosyl-2,5-dihydro-1H-pyrrol-3-yl)-2,2-dimethylpropan-1-one (4ff): 128.4 mg, 79%; white solid (mp. 144.8–145.3 °C); ¹H NMR (400 MHz, CDCl₃, 25 °C) δ 0.96 (s, 9 H), 1.09 (s, 9 H), 2.52 (s, 3 H), 3.90 (ddd, *J* = 15.6, 6.0, 3.6 Hz, 1 H), 4.23 (ddd, *J* = 15.6, 6.0, 2.8 Hz, 1 H), 4.34

(ddd, $J = 13.2, 6.0, 3.6$ Hz, 1 H), 4.61 (ddd, $J = 13.2, 6.0, 2.8$ Hz, 1 H), 6.32 (s, 1 H), 6.86 (d, $J = 8.4$ Hz, 2 H), 7.10 (d, $J = 8.4$ Hz, 2 H), 7.37 (d, $J = 8.0$ Hz, 2 H), 7.66 (d, $J = 8.0$ Hz, 2 H); ^{13}C NMR (100 MHz, CDCl_3 , 25 °C) δ 21.7, 25.8, 30.2, 36.8, 43.8, 55.7, 57.8, 120.5, 124.8, 127.5, 129.5, 130.1, 131.2, 133.1, 133.2, 136.0, 144.2, 144.7, 145.8, 202.7; IR (neat) 1680 (C=O) cm^{-1} ; HRMS (ESI) m/z calcd for $\text{C}_{28}\text{H}_{34}\text{BrNO}_3\text{S}\cdot\text{Na}$ 566.1341, found 566.1324 $[\text{M}+\text{Na}]^+$.

Analytical data for

**(Z)-1-(4-(3,3-dimethyl-1-(thiophen-2-yl)but-1-en-2-yl)-1-tosyl-2,5-dihydro-1H-pyrro-
l-3-yl)-2,2-dimethylpropan-1-one (4fi):** 97.8 mg, 69%; white solid (mp. 164.1–
165.3 °C); ^1H NMR (400 MHz, CDCl_3 , 25 °C) δ 1.05 (s, 9 H), 1.08 (s, 9 H), 2.47 (s, 3
H), 4.16 (dt, $J = 15.6, 4.8$ Hz, 1 H), 4.24 (ddd, $J = 15.6, 5.6, 2.6$ Hz, 1 H), 4.52 (dt, $J =$
13.6, 4.8 Hz, 1 H), 4.77 (ddd, $J = 13.6, 5.6, 2.6$ Hz, 1 H), 6.57 (s, 1 H), 6.78–6.80 (m, 3
H), 7.33 (d, $J = 8.4$ Hz, 2 H), 7.76 (d, $J = 8.4$ Hz, 2 H); ^{13}C NMR (100 MHz, CDCl_3 ,
25 °C) δ 21.6, 26.0, 30.2, 36.5, 44.0, 56.3, 57.0, 119.7, 125.2, 126.2, 127.8, 129.9, 133.4,
134.3, 139.7, 141.2, 143.8, 145.5, 201.7; IR (neat) 1680 (C=O) cm^{-1} ; HRMS (ESI)
 m/z calcd for $\text{C}_{26}\text{H}_{33}\text{NO}_3\text{S}_2\cdot\text{Na}$ 494.1799, found 494.1800 $[\text{M}+\text{Na}]^+$.

Analytical data for
1-(4-((3E,5E)-6-(4-methoxyphenyl)-2,2-dimethylhexa-3,5-dien-3-yl)-1-tosyl-2,5-dihydro-1H-pyrrol-3-yl)-2,2-dimethylpropan-1-one (4fj): 131.0 mg, 81%; dark-brown paste; ¹H NMR (400 MHz, CDCl₃, 25 °C) δ 1.04 (s, 9 H), 1.06 (s, 9 H), 2.42 (s, 3 H), 4.09 (ddd, *J* = 15.6, 5.8, 3.4 Hz, 1 H), 4.28 (ddd, *J* = 16.0, 5.4, 3.0 Hz, 1 H), 3.32 (s, 3 H), 4.53 (ddd, *J* = 13.6, 5.6, 3.2 Hz, 1 H), 4.64 (ddd, *J* = 13.6, 5.6, 3.2 Hz, 1 H), 6.14 (d, *J* = 11.0 Hz, 1 H), 6.24 (dd, *J* = 14.8, 11.0 Hz, 1 H), 6.42 (d, *J* = 14.8 Hz, 1 H), 6.82 (d, *J* = 8.8 Hz, 2 H), 7.13 (d, *J* = 8.8 Hz, 2 H), 7.36 (d, *J* = 8.0 Hz, 2 H), 7.78 (d, *J* = 8.0 Hz, 2 H); ¹³C NMR (100 MHz, CDCl₃, 25 °C) δ 21.6, 26.1, 30.3, 35.7, 44.1, 55.3, 56.4, 58.8, 114.0, 123.6, 126.6, 127.5, 127.6, 129.9, 130.0, 132.5, 133.4, 143.5, 143.6, 144.0, 159.2, 203.8; IR (neat) 1687 (C=O) cm⁻¹; HRMS (ESI) *m/z* calcd for C₃₁H₃₉NO₄S•Na 544.2498, found 544.2477 [M+Na]⁺.

Reaction of Diynes with DMF.

General procedure – Synthesis of (3E,4Z)-dimethyl 3-benzylidene-4-(2-(dimethylamino)-2-oxo-1-phenylethylidene)cyclopentane-1,1-dicarboxylate (6m): A solution of diyne **2m** (108.0 mg, 0.300 mmol) and catalyst **1b**

(13.0 mg, 0.030 mmol) in dry DMF (1.0 mL) was degassed at $-78\text{ }^{\circ}\text{C}$ and backfilled with argon (three times). The reaction mixture was stirred at $140\text{ }^{\circ}\text{C}$ for 30 min. After concentration in *vacuo*, the crude product was purified by flash column chromatography on silica gel (hexane/AcOEt, 10:1~1:1) to afford **6m** (91.3 mg, 70%) as a pale-yellow solid ($111.8\text{ }^{\circ}\text{C}$ decomp):⁸ ^1H NMR (400 MHz, CDCl_3 , $25\text{ }^{\circ}\text{C}$) δ 3.02 (s, 3 H), 3.05 (s, 3 H), 3.00–3.54 (m, 4 H), 3.69 (br s, 6 H), 6.88 (t, $J = 2.6\text{ Hz}$, 1 H), 7.22–7.40 (m, 10 H); ^{13}C NMR (100 MHz, CDCl_3 , $25\text{ }^{\circ}\text{C}$) δ 34.6, 37.5, 39.0, 39.3, 52.9, 57.5, 126.5, 127.3, 127.8, 128.3, 128.4, 128.5, 129.1, 130.2, 136.5, 137.28, 137.30, 137.4, 170.6.

Analytical data for
(Z)-2-((E)-4,4-diacetyl-2-benzylidenecyclopentylidene)-N,N-dimethyl-2-phenylacetamide (6n): 94.3 mg, 78%; pale-yellow solid (mp $67.4\text{--}71.3\text{ }^{\circ}\text{C}$); ^1H NMR (400 MHz, CDCl_3 , $25\text{ }^{\circ}\text{C}$) δ 2.07 (s, 6 H), 2.99 (s, 3 H), 3.00 (s, 3 H), 2.90–3.50 (m, 4 H), 6.85 (t, $J = 2.4\text{ Hz}$, 1 H), 7.26–7.41 (m, 10 H); ^{13}C NMR (100 MHz, CDCl_3 , $25\text{ }^{\circ}\text{C}$) δ 26.4/26.8 (br s), 34.5, 36.1, 36.7, 37.6, 71.8, 126.7, 127.4, 127.9, 128.3, 128.5, 128.6, 129.1, 130.5, 136.7, 137.15, 137.21, 170.4, 204.5 (br s); IR (neat) 1699 (C=O) , 1620 (C=O) cm^{-1} ; HRMS (ESI) m/z calcd for $\text{C}_{26}\text{H}_{27}\text{NO}_3\cdot\text{Na}$ 424.1889, found 424.1891

[M+Na]⁺.

Analytical data for

(Z)-2-((E)-3-benzylidene-6,10-dioxospiro[4.5]decan-2-ylidene)-N,N-dimethyl-2-phenylacetamide (6o): 93.2 mg, 75%; white solid (mp 161.2–163.7 °C); ¹H NMR (400 MHz, CDCl₃, 25 °C) δ 1.94 (quint, *J* = 6.7 Hz, 2 H), 2.58–2.72 (m, 4 H), 2.97 (br s, 2 H), 3.01 (s, 3 H), 3.10 (s, 3 H), 3.24 (d, *J* = 2.8 Hz, 2 H), 6.87 (t, *J* = 2.8 Hz, 1 H), 7.22–7.40 (m, 10 H); ¹³C NMR (100 MHz, CDCl₃, 25 °C) δ 17.6, 34.6, 36.8, 37.3/38.0 (br s), 37.7, 38.3, 69.5, 126.2, 127.2, 127.7, 128.3, 128.4, 128.5, 129.1, 129.8, 136.8, 137.3, 137.5, 137.7, 170.5, 206.5/207.8 (br s); IR (neat) 1695 (C=O), 1618 (C=O) cm⁻¹; HRMS (ESI) *m/z* calcd for C₂₇H₂₇NO₃•Na 436.1889, found 436.1910 [M+Na]⁺.

Analytical data for

(Z)-2-((E)-2-benzylidene-4,4-bis(methoxymethyl)cyclopentylidene)-N,N-dimethyl-2-phenylacetamide (6p): 82.4 mg, 68%; colorless paste; ¹H NMR (400 MHz, CDCl₃, 25 °C) δ 2.40 (br d, *J* = 15.6 Hz, 1 H), 2.59 (br d, *J* = 15.6 Hz, 1 H), 2.69 (d, *J* = 4.8 Hz, 2 H), 3.00 (s, 3 H), 3.54 (s, 3 H), 3.15–3.35 (br m, 10 H), 6.84 (t, *J* = 2.4 Hz, 1 H), 7.21–7.41 (m, 10 H); ¹³C NMR (100 MHz, CDCl₃, 25 °C) δ 34.5, 37.5, 37.6, 37.7,

45.4, 59.2, 75.8/76.1 (br s), 125.8, 126.9, 127.4, 128.2, 128.3, 129.1, 129.6, 137.7, 137.9, 139.9, 140.2, 171.1; IR (neat) 1622 (C=O) cm^{-1} ; HRMS (ESI) m/z calcd for $\text{C}_{26}\text{H}_{31}\text{NO}_3 \cdot \text{Na}$ 428.2202, found 428.2221 $[\text{M}+\text{Na}]^+$.

Analytical data for (3E,4Z)-ethyl 3-benzylidene-4-(2-(dimethylamino)-2-oxo-1-phenylethylidene)cyclopentanecarboxylate (6q):⁸ 78.3 mg, 70%; pale-yellow solid (mp 119.1–119.8 °C); ^1H NMR (400 MHz, CDCl_3 , 25 °C) δ 1.22 (t, $J = 7.0$ Hz, 3 H), 2.70–3.15 (m, 11 H), 4.12 (q, $J = 7.0$ Hz, 2 H), 6.86 (t, $J = 2.4$ Hz, 1 H), 7.22–7.45 (m, 10 H); ^{13}C NMR (100 MHz, CDCl_3 , 25 °C) δ 14.1, 34.5, 35.8, 37.4, 41.7, 60.7, 125.7, 127.1, 127.6, 128.3, 128.4, 129.1, 129.7, 137.4, 137.6, 138.8, 170.7, 175.1.

Analytical data for (Z)-2-((E)-4-acetyl-2-benzylidenecyclopentylidene)-N,N-dimethyl-2-phenylacetamide (6r):⁸ 75.6 mg, 70%; pale-yellow solid (mp 176.4 °C decomp); ^1H NMR (400 MHz, CDCl_3 , 25 °C) δ 2.16 (s, 3 H), 2.64–3.12 (m, 11 H), 6.85 (br s, 1 H), 7.22–7.45 (m, 10 H); ^{13}C NMR (100 MHz, CDCl_3 , 25 °C) δ 29.3, 34.6, 34.8, 37.5, 49.5, 125.7, 127.2, 127.7, 128.3, 128.5, 129.1, 129.9, 137.4, 137.7, 138.8, 138.9, 170.7, 209.4.

DFT Calculations

The Gaussian 09 program package was used for all geometry optimizations.¹⁵ The geometries of the stationary points and transition states were fully optimized using the Becke's three-parameter hybrid density functional method (B3LYP)¹⁶ with a double- ζ basis set with the relativistic effective core potential of Hay and Wadt (LanL2DZ)¹⁷ for Ru and the 6-31G(d)¹⁸ basis sets for other elements. The vibrational frequencies and thermal correction to Gibbs free energy (TCGFE) including zero-point energy were calculated at the same level of theory. The obtained structures were characterized by the number of imaginary frequencies (IF, one or zero for transition or ground states, respectively). The connectivity of each step was also confirmed by intrinsic reaction coordinate (IRC) calculation¹⁹ from the transition states followed by optimization of the resultant geometries. Single-point energies for geometries obtained by the above method were calculated using the Truhlar's M06L functional²⁰ with the basis sets consisting of a [6s5p3d2f1g] contracted valence basis set with the Stuttgart-Dresden-Bonn energy-consistent pseudopotential (SDD)^{21,22} for Ru and the 6-311++G(d,p) basis sets²³ for other elements. To examine the solvent effect, the above

single-point energy calculations were performed using the polarizable continuum model (PCM)²⁴ method with dielectric constants (ϵ) of 7.4257 for THF. The obtained energies, ZPEs, TCGFEs, and IF are summarized in Tables S1.

ASSOCIATED CONTENT

Supporting Information

The Supporting Information is available free of charge on the ACS Publication website.

Table S1 and ¹H and ¹³C NMR charts (PDF)

Cartesian coordinates of calculated molecules (XYZ)

AUTHOR INFORMATION

Corresponding Author

*E-mail: yamamoto-yoshi@ps.nagoya-u.ac.jp

Notes

The authors declare no competing financial interest.

ACKNOWLEDGMENTS

This research is partially supported by the Platform Project for Supporting Drug Discovery and Life Science Research (AMED) and JSPS KAKENHI (Grand Number JP 16KT0051).

REFERENCES

- (1) For recent comprehensive reviews, see: (a) Kotha, S.; Brahmachary, E.; Lahiri, K. *Eur. J. Org. Chem.* **2005**, 4741-4767. (b) Chopade, P. R.; Louie, J. *Adv. Synth. Catal.* **2006**, *348*, 2307-2327. (c) Agenet, N.; Buisine, O.; Slowinski, F.; Gandon, V.; Aubert, C.; Malacria, M. *Org. React.* **2007**, *68*, 1-302. (d) Domínguez, G.; Pérez-Castells, J. *Chem. Soc. Rev.* **2011**, *40*, 3430-3444. (e) Broere, D. L.; Ruijter, E. *Synthesis* **2012**, *44*, 2639-2672.
- (2) For reviews, see: (a) Heller, B.; Hapke, M. *Chem. Soc. Rev.* **2007**, *36*, 1085-1094. (b) Varela, J. A.; Saá, C. *Synlett* **2008**, 2571-2578. (c) Shaaban, M. R.; El-Sayed, R.; Elwahy, A. H. M. *Tetrahedron* **2011**, *67*, 6095-6130.
- (3) (a) Tsuda, T.; Kiyoi, T.; Miyane, T.; Saegusa, T. *J. Am. Chem. Soc.* **1988**, *110*,

- 8570-8572. (b) Tekevac, T. N.; Louie, J. *Org. Lett.* **2005**, *7*, 4037-4039.
- (4) (a) Harvey, D. F.; Johnson, B. M.; Ung, C. S.; Vollhardt, K. P. C. *Synlett* **1989**, 15-18. (b) Takahashi, T.; Li, Y.; Ito, T.; Xu, F.; Nakajima, K.; Liu, Y. *J. Am. Chem. Soc.* **2002**, *124*, 1144-1145.
- (5) (a) Tsuchikama, K.; Yoshinami, Y.; Shibata, T. *Synlett* **2007**, 1395-1398. (b) Otake, Y.; Tanaka, R.; Tanaka, K. *Eur. J. Org. Chem.* **2009**, 2737-2747.
- (6) The rhodium-catalyzed fully intramolecular [2 + 2 + 2] reaction of allene-alkyne-aldehydes was reported, see: Oonishi, Y.; Kitano, Y.; Sato, Y. *Tetrahedron* **2013**, *69*, 7713-7718.
- (7) Yamamoto, Y.; Takagishi, H.; Itoh, K. *J. Am. Chem. Soc.* **2002**, *124*, 6844-6845.
- (8) Mori, S.; Shibuya, M.; Yamamoto, Y. *Chem. Lett.* **2017**, *46*, 207-210.
- (9) Evanseck, J. D.; Thomas, B. E., IV; Spellmeyer, D. C.; Houk, K. N. *J. Org. Chem.* **1995**, *60*, 7134-7141.
- (10) (a) Yamamoto, Y.; Arakawa, T.; Ogawa, R.; Itoh, K. *J. Am. Chem. Soc.* **2003**, *125*, 12143-12160. (b) Yamamoto, Y.; Kinpara, K.; Saigoku, T.; Takagishi, H.; Okuda, S.; Nishiyama, H.; Itoh, K. *J. Am. Chem. Soc.* **2005**, *127*, 605-613. (c) Kirchner,

K.; Calhorda, M. J.; Schmid, R.; Veiros, L. F. *J. Am. Chem. Soc.* **2003**, *125*, 11721-11729. (d) Rüba, E.; Schmid, R.; Kirchner, K.; Calhorda, M. J. *J. Organomet. Chem.* **2003**, *682*, 204-211. (e) Schmid, R.; Kirchner, K. *J. Org. Chem.* **2003**, *68*, 8339-8344.

(11) Tekavec, T. N.; Arif, A. M.; Louie, J. *Tetrahedron* **2004**, *60*, 7431-7437.

(12) Yamamoto, Y. *Organometallics* **2017**, *36*, 1154-1163.

(13) (a) Scheller, A.; Winter, W.; Müller, E. *Liebigs Ann. Chem.* **1976**, 1448-1454. (b)

Atkinson, R. S.; Grimshire, M. J. *J. Chem. Soc., Perkin Trans. 1* **1986**, 1215-1224.

(c) Louie, J.; Gibby, J. E.; Farnworth, M. V.; Tekavec, T. N. *J. Am. Chem. Soc.*

2002, *124*, 15188-15189. (d) Mulin, S.; Dentel, H.; Pagnoux-Ozherelyeva, A.;

Gaillard, S.; Poater, A.; Cavallo, L.; Lohier, J.-F.; Renaud, J.-L. *Chem. Eur. J.*

2013, *19*, 17881-17890. (e) Richard, V.; Ipouck, M.; Mérel, D. S.; Gaillard, S.;

Whitby, R. J.; Witulski, B.; Renaud, J.-L. *Chem. Commun.* **2014**, *50*, 593. (f) Jang,

H.-Y.; Krische, M. J. *J. Am. Chem. Soc.* **2004**, *126*, 7875-7880. (g) Hu, Y.; Sun,

Y.; Hu, J.; Zhu, T.; Yu, T.; Zhao, Q. *Chem. Asian J.* **2011**, *6*, 797-800. (h) Bedi,

A.; Debnath, S.; Chandak, H. S.; Zade, S. S. *RSC Adv.* **2014**, *4*, 35653-35658.

- (14) (a) Kündig, E. P.; Monnier, F. R. *Adv. Synth. Catal.* **2004**, *346*, 901-904. (b)
Steinmetz, B.; Schenk, W. A. *Organometallics* **1999**, *18*, 943-946.
- (15) Gaussian 09, Revision C.01, Frisch, M. J.; Trucks, G. W.; Schlegel, H. B.;
Scuseria, G. E.; Robb, M. A.; Cheeseman, J. R.; Scalmani, G.; Barone, V.;
Mennucci, B.; Petersson, G. A.; Nakatsuji, H.; Caricato, M.; Li, X.; Hratchian, H.
P.; Izmaylov, A. F.; Bloino, J.; Zheng, G.; Sonnenberg, J. L.; Hada, M.; Ehara, M.;
Toyota, K.; Fukuda, R.; Hasegawa, J.; Ishida, M.; Nakajima, T.; Honda, Y.; Kitao,
O.; Nakai, H.; Vreven, T.; Montgomery, Jr., J. A.; Peralta, J. E.; Ogliaro, F.;
Bearpark, M.; Heyd, J. J.; Brothers, E.; Kudin, K. N.; Staroverov, V. N.;
Kobayashi, R.; Normand, J.; Raghavachari, K.; Rendell, A.; Burant, J. C.; Iyengar,
S. S.; Tomasi, J.; Cossi, M.; Rega, N.; Millam, J. M.; Klene, M.; Knox, J. E.;
Cross, J. B.; Bakken, V.; Adamo, C.; Jaramillo, J.; Gomperts, R.; Stratmann, R.
E.; Yazyev, O.; Austin, A. J.; Cammi, R.; Pomelli, C.; Ochterski, J. W.; Martin, R.
L.; Morokuma, K.; Zakrzewski, V. G.; Voth, G. A.; Salvador, P.; Dannenberg, J.
J.; Dapprich, S.; Daniels, A. D.; Farkas, Ö.; Foresman, J. B.; Ortiz, J. V.;
Cioslowski, J.; Fox, D. J., Gaussian, Inc., Wallingford CT, 2009.

- (16) (a) Kohn, W.; Becke, A. D.; Parr, R. G. *J. Phys. Chem.* **1996**, *100*, 12974-12980.
(b) Stephens, P. J.; Devlin, F. J.; Chabalowski, C. F.; Frisch, M. J. *J. Phys. Chem.* **1994**, *98*, 11623-11627. (c) Becke, A. D. *J. Chem. Phys.* **1993**, *98*, 5648-5652. (d) Lee, C.; Yang, W.; Parr, R. G. *Phys. Rev. B* **1988**, *37*, 785-789.
- (17) Hay, P. J.; Wadt, W. R. *J. Chem. Phys.* **1985**, *82*, 299-310.
- (18) (a) Hehre, W. J.; Ditchfield, R.; Pople, J. A. *J. Chem. Phys.* **1972**, *56*, 2257-2261.
(b) Hariharan, P. C.; Pople, J. A. *Theor. Chim. Acta* **1973**, *28*, 213-222. (c) Frack, M. M.; Pietro, W. J.; Hehre, W. J.; Binkley, J. S.; Gordon, M. S.; DeFrees, D. J.; Pople, J. A. *J. Chem. Phys.* **1982**, *77*, 3654-3665.
- (19) (a) Fukui, K. *Acc. Chem. Res.* **1981**, *14*, 363-368. (b) Gonzalez, C.; Schlegel, H. B. *J. Chem. Phys.* **1989**, *90*, 2154-2161. (c) Gonzalez, C.; Schlegel, H. B. *J. Phys. Chem.* **1990**, *94*, 5523-5527.
- (20) Zhao, Y.; Truhlar, D. G. *Acc. Chem. Res.* **2008**, *41*, 157-167
- (21) Martin, J. M. L.; Sundermann, A. *J. Chem. Phys.* **2001**, *114*, 3408-3420.
- (22) Andrae, D.; Häussermann, U.; Dolg, M.; Stoll, H.; Preuß, H. *Theor. Chim. Acta* **1990**, *77*, 123-141.

- (23) (a) Krishnan, R.; Binkley, J. S.; Seeger, R.; Pople, J. A. *J. Chem. Phys.* **1980**, *72*, 650-654. (b) McLean, A. D.; Chandler, G. S. *J. Chem. Phys.* **1980**, *72*, 5639-5648. (c) Frisch, M. J.; Pople, J. A.; Binkley, J. S. *J. Chem. Phys.* **1984**, *80*, 3265-3269. (d) Clark, T.; Chandrasekhar, J.; Spitznagel, G. W.; Schleyer, P. v. R. *J. Comp. Chem.* **1983**, *4*, 294-301.
- (24) (a) Miertuš, S.; Scrocco, E.; Tomasi, J. *Chem. Phys.* **1981**, *55*, 117-129. (b) Pascual-Ahuir, J. L.; Silla, E.; Tomasi, J.; Bonaccorsi, R. *J. Comput. Chem.* **1987**, *8*, 778-787. (c) Floris, F.; Tomasi, J. *J. Comput. Chem.* **1989**, *10*, 616-627. (d) Cossi, M.; Barone, V.; Cammi, R.; Tomasi, J. *Chem. Phys. Lett.* **1996**, *255*, 327-335. (e) Cancès, E.; Mennucci, B.; Tomasi, J. *J. Chem. Phys.* **1997**, *22*, 3032-3041. (f) Barone, V.; Cossi, M.; Tomasi, J. *J. Chem. Phys.* **1997**, *22*, 3210-3221.